

The authors are grateful to the anonymous referee #2 who gave his/her time to provide helpful comments and suggestions that improved our manuscript. Here, we present the answers for each of the comments. The manuscript and supplement with tracked changes can be found at the end of the document.

- 5 ▪ **The writing of the paper obscured the fact that the observations were not continuous. The dataset includes ~ 1 month in winter, spring, and summer and 3 months in autumn. Some of the differences in comparison to other studies may be due to the comparison of 1 month data to a season.**

10 Authors' response: The information about the investigation period is now clearly mentioned in the abstract, introduction, and methods sections. Besides, the time series plot (Figure 1) also shows the observation period clearly and it is mentioned in section 3.1. Comparison with other studies is now done carefully. The observation periods of the previous studies are also mentioned in the text. Most of the previous studies we presented in our comparison discussion did not present any time series plot for the whole observation period and also did not mention clearly
15 that the measurement was continuously performed for a season or a year. So, it is not certain that we are comparing our 1-3 months data to a season.

- 20 ▪ **I do not suggest including halocarbons in TVOC comparison. Halocarbons are not reactive and do not contribute significantly to OH reactive or the productions of ozone and SOA. There are good reasons for not including halocarbons in TVOC data in previous studies. In the discussion of Line 250-260, it is unclear if and what halocarbons and OVOCs were included in TVOCs in previous studies. Not knowing that, the comparison results can be misleading.**

25 Authors' response: Many previous studies also included halocarbons in TVOC estimation and we already included those reported TVOC concentrations in our comparison discussion (e.g. Li et al., 2015; Zhang et al., 2018; Zeng et al., 2018; Sun et al., 2019). We still want to compare our observation with these studies. That is why we are now reporting TVOC concentration with halocarbons and without halocarbons. Now we have rewritten the TVOC comparison part. We checked carefully each previous study to find out what kind of VOCs they included in their TVOC estimation and the comparison with our observation is done accordingly. Moreover,
30 OVOCs are also not included in TVOC estimation in several studies (e.g. Zhang et al., 2018; Jia

et al., 2016; Hui et al., 2018; Liu et al., 2016a; Mo et al., 2017; Song et al., 2018). That is why we also estimated TVOC without OVOCs and compare it with those studies.

- 35
- **The discussion of section 3.3.1 can be removed. T/B ratio is meaningful only if they are from a single source. The PMF results show that T and B are from multiple sources and T/B ratio is not meaning. The same argument applies to the ratios of alkanes or aromatics to acetylene.**

Authors' response: Section 3.3.1 is removed.

- 40
- **The PMF results are confusing. In summer, for example, ethane is from vehicle, isopentane is from biogenic sources, ethane and propane are from vehicles, and propane is from solvent use. None of these make much sense. It's more or less the same for other seasons. In autumn, biomass burning has ethane but not acetylene. In winter, vehicle 1 and 2 are similar. Spring and autumn have gasoline**
- 45
- **evaporation, but summer and winter do not. Gasoline evaporation should be largest in summer. LPG/NP does not have ethylene in spring but has most of ethylene in winter.**

Authors' response: PMF model analysis is carried out again using typical tracers of various emission sources and the text has been modified accordingly.

- 50
- **PSFC analysis is applicable only to VOCs that are short lived because the backtrajectories are only 24 hours.**

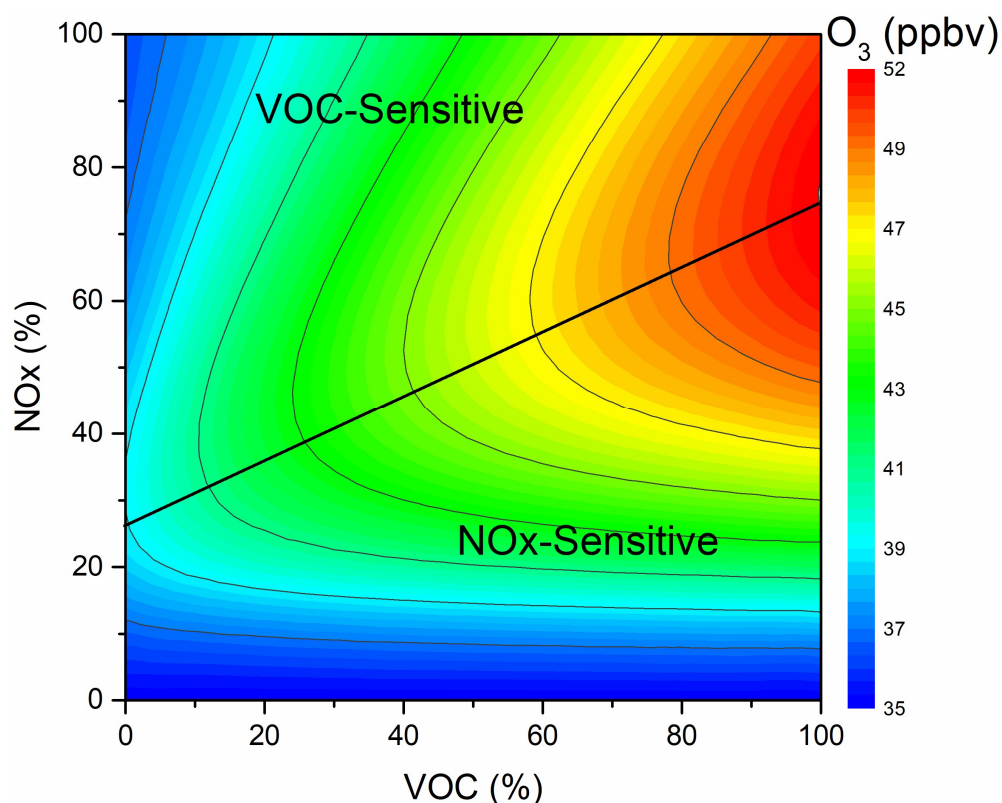
Authors' response: New PSCF analysis based on 72 hours backward air mass trajectories is now added. The text has been modified according to the new PSCF analysis.

- 55
- **I do not feel OFP and SOAP analyses are useful (although they are often included in VOC papers). Figures 7 and 8 show that VOCs have much higher OFP and SOAP in winter than summer, which is technically true but we know the contributions of VOCs to ozone and SOA are much larger in summer than winter.**

60 Authors' response: The OFP and SOAP analyses are removed.

- 65 **▪ The EKMA diagrams of Figure 10 show ozone at ~50 ppbv for 100% NO_x and VOCs in summer. Ozone here is daily 1 hour maximum, I think. 50 ppbv seems low for daily 1 hour maximum in summer. One possible reason is that the Thermo chemiluminescence instrument can severely overestimate NO₂ because of the conversion of NO_y to NO_x.**

Response: Yes, the Thermo chemiluminescence instrument can overestimate NO₂ concentrations (Dunlea et al., 2007). However, there is also evidence that it does not significantly overestimate NO₂ concentrations (Chate et al., 2014). Anyway, following Dunlea et al. (2007), we ran the box model using NO₂ concentrations reduced by 22% and made the summertime EKMA diagram (Figure R1 below). However, the 1-hour maximum O₃ concentration for 100% NO_x and VOCs did not increase.



75 Figure R1: O₃ isopleth diagram for summer based on percentage changes in VOCs and NO_x concentrations in Nanjing and corresponding modelled O₃ production. In the model input, the NO₂ concentrations were reduced by 22%.

- **“Halocarbons” was mis-spelled in several places.**

Authors’ response: Amended. The term “halocarbon” is used everywhere instead of “halohydrocarbon”.

80

References

- Chate, D. M., Ghude, S. D., Beig, G., Mahajan, A. S., Jena, C., Srinivas, R., ... Kumar, N. (2014). Deviations from the O₃-NO-NO₂ photo-stationary state in Delhi, India. *Atmospheric Environment*, *96*(2), 353–358. <https://doi.org/10.1016/j.atmosenv.2014.07.054>
- 85 Dunlea, E. J., Herndon, S. C., Nelson, D. D., Volkamer, R. M., San Martini, F., Sheehy, P. M., ... Molina, M. J. (2007). Evaluation of nitrogen dioxide chemiluminescence monitors in a polluted urban environment. *Atmospheric Chemistry and Physics*, *7*(10), 2691–2704. <https://doi.org/10.5194/acp-7-2691-2007>
- Hui, L., Liu, X., Tan, Q., Feng, M., An, J., Qu, Y., ... Jiang, M. (2018). Characteristics, source apportionment and contribution of VOCs to ozone formation in Wuhan, Central China. *Atmospheric Environment*, *192*(2), 55–71. <https://doi.org/10.1016/j.atmosenv.2018.08.042>
- 90 Jia, C., Mao, X., Huang, T., Liang, X., Wang, Y., Shen, Y., ... Gao, H. (2016). Non-methane hydrocarbons (NMHCs) and their contribution to ozone formation potential in a petrochemical industrialized city, Northwest China. *Atmospheric Research*, *169*, 225–236. <https://doi.org/10.1016/j.atmosres.2015.10.006>
- 95 Li, J., Xie, S. D., Zeng, L. M., Li, L. Y., Li, Y. Q., & Wu, R. R. (2015). Characterization of ambient volatile organic compounds and their sources in Beijing, before, during, and after Asia-Pacific Economic Cooperation China 2014. *Atmospheric Chemistry and Physics*, *15*(14), 7945–7959. <https://doi.org/10.5194/acp-15-7945-2015>
- 100 Liu, B., Liang, D., Yang, J., Dai, Q., Bi, X., Feng, Y., ... Xu, H. (2016). Characterization and source apportionment of volatile organic compounds based on 1-year of observational data in Tianjin, China. *Environmental Pollution*, *218*, 757–769. <https://doi.org/10.1016/j.envpol.2016.07.072>
- Mo, Z., Shao, M., Lu, S., Niu, H., Zhou, M., & Sun, J. (2017). Characterization of non-methane

105 hydrocarbons and their sources in an industrialized coastal city , Yangtze River Delta ,
China. *Science of the Total Environment*, 593–594, 641–653.
<https://doi.org/10.1016/j.scitotenv.2017.03.123>

Song, M., Tan, Q., Feng, M., Qu, Y., & Liu, X. (2018). Source Apportionment and Secondary
Transformation of Atmospheric Nonmethane Hydrocarbons in Chengdu , Southwest China.
110 *Journal of Geophysical Research Atmospheres*, 123(2), 9741–9763.
<https://doi.org/10.1029/2018JD028479>

Sun, J., Shen, Z., Zhang, Y., Zhang, Z., Zhang, Q., Zhang, T., ... Li, X. (2019). Urban VOC
profiles, possible sources, and its role in ozone formation for a summer campaign over
Xi'an, China. *Environmental Science and Pollution Research*, 26(27), 27769–27782.
115 <https://doi.org/10.1007/s11356-019-05950-0>

Zeng, P., Lyu, X. P., Guo, H., Cheng, H. R., Jiang, F., Pan, W. Z., ... Hu, Y. Q. (2018). Causes
of ozone pollution in summer in Wuhan, Central China. *Environmental Pollution*, 241(x),
852–861. <https://doi.org/10.1016/j.envpol.2018.05.042>

Zhang, Y., Li, R., Fu, H., Zhou, D., & Chen, J. (2018). Observation and analysis of atmospheric
120 volatile organic compounds in a typical petrochemical area in Yangtze River. *Journal of
Environmental Sciences*, 71, 233–248. <https://doi.org/10.1016/j.jes.2018.05.027>

125

130

135

Measurement report: High Contributions of Halocarbon and Aromatic Compounds to Emissions and Chemistry of Atmospheric VOCs in Industrial Area

Ahsan Mozaffar^{1,2,3}, Yan-Lin Zhang^{1,2,3*}, Yu-Chi Lin^{1,2,3}, Feng Xie^{1,2,3}, Mei-Yi Fan^{1,2,3}, and Fang Cao^{1,2,3}

140 ¹Yale-NUIST Center on Atmospheric Environment, International Joint Laboratory on Climate and Environment Change, Nanjing University of Information Science and Technology, Nanjing, 210044, China.

²Key Laboratory Meteorological Disaster; Ministry of Education & Collaborative Innovation Center on Forecast and Evaluation of Meteorological Disaster, Nanjing University of Information Science and Technology, Nanjing, 210044, China.

³Jiangsu Provincial Key Laboratory of Agricultural Meteorology, College of Applied Meteorology, Nanjing University of Information Science & Technology, Nanjing 210044, China.

Correspondence to: Yan-Lin Zhang (dryanlinzhang@outlook.com)

Abstract. Volatile organic compounds (VOCs) are key components for tropospheric chemistry and air quality. We investigated ambient VOCs in an industrial area in Nanjing, China for about 1 month in winter, spring, and summer and 3 months in autumn from-between July 2018 ~~to and~~ May 2020. The total VOCs (TVOCs) concentration was 59.8 ± 28.6 ppbv during the investigation period. About twice TVOCs concentrations were observed in autumn (83 ± 20 ppbv) and winter (77.5 ± 16.8 ppbv) seasons compared to those in spring (39.6 ± 13.1 ppbv) and summer (38.8 ± 10.2 ppbv). Unlike-In previous studies in Nanjing, oxygenated-VOCs (OVOCs) and halocarbons were not measured, ~~the observed TVOCs was about 1.5 and 3 times higher than those previously reported in the same study area and a nonindustrial suburban area in Nanjing, respectively the current TVOCs concentration without halocarbons and OVOCs was similar to the previous investigation in the same study area, however, 2 folds higher than the one reported in the nonindustrial suburban area in Nanjing.~~ Observed TVOCs concentrations ~~were~~ was similar to ~~those the one in the~~ metropolitan city Beijing, ~~and but,~~ 1.3 fold smaller than the one reported in Shanghai. Observed TVOCs concentration was similar to those in Lanzhou, Chengdu, Tokyo, and Xi'an, however, it was about 1.5-~~3~~-1.7 folds higher than those in ~~Lanzhou,~~ Wuhan, Tianjin, ~~and~~ Ningbo, ~~Chengdu, London, Los Angeles, and Tokyo.~~ Due to the industrial influence,

165 halocarbons (14.3 ± 7.3 ppbv, 24%) VOC-group was the second largest contributor to the TVOCs
after alkanes (21 ± 7 ppbv, 35%), which is in contrast with the previous studies in Nanjing and
also in almost other regions in China. Relatively high proportions of haloalkanes and
aromatics were observed in autumn (25.7 and 19.3%, respectively) and winter (25.8 and 17.6%,
170 13.6%, respectively). According to the potential source contribution function (PSCF), short-
distance transports from the surrounding industrial areas and cities were the main reason for high
VOC concentration in the study area. According to positive matrix factorization (PMF) model
results, ~~industry-related sources (23–47%) followed by~~ vehicle-related emissions (24.3–34.48%)
175 contributed the major portion to the ambient VOC concentrations. ~~Whereas aromatics~~ Aromatics
followed by alkenes were the top contributors to the loss rate of OH radicals (L^{OH}) (37 and 32%,
respectively), ~~alkenes followed by aromatics contributed most to the ozone formation potential~~
~~(OFP) (39 and 28%, respectively). Besides, the aromatics VOC group was also the major~~
~~contributor to the secondary organic aerosol potential (SOAP) (97%).~~ According to the empirical
kinetic modelling approach (EKMA) and relative incremental reactivity (RIR) analysis in
180 assistance with a photochemical box model, the study area was in the VOC-sensitive regime for
ozone (O_3) formation during all the measurements seasons. Therefore, mainly alkenes and
aromatics emissions chiefly from ~~industries and~~ automobiles should be reduced to decrease the
secondary air pollution formation in the study area.

1 Introduction

185 Air pollution characterized by severe ozone (O_3) and haze pollution is a big problem in urban
and industrial areas in China (He et al., 2019; Hui et al., 2018; Tan et al., 2018; Jia et al., 2016;
Feng et al., 2016; Hui et al., 2019). In recent years, O_3 concentration above the national standard,
and severe haze events are frequently reported (He et al., 2019; Hui et al., 2019; Sheng et al.,
2018; Feng et al., 2016; Tan et al., 2018; Jia et al., 2016). As a precursor of O_3 and secondary
190 organic aerosol (SOA), volatile organic compounds (VOCs) are largely responsible for the
severe air pollution in China (Song et al., 2018; Hui et al., 2019; Hui et al., 2018; He et al.,
2019). Unfortunately, anthropogenic VOC emissions have been increasing over the last 2
decades in China and it is expected to do so in the future (Mozaffar & Zhang, 2020, and
references therein).

195 Atmospheric VOC has plenty of sources; it can be emitted from various anthropogenic and biogenic sources. Besides, it can also be formed in the atmosphere. Anthropogenic VOC sources mainly include industrial emission, vehicle exhaust, solvent usages, biomass burning, and fuel evaporation. On the other hand, vegetation is the main biogenic sources of VOC. In developed areas in China, vehicle exhaust and industrial emission are the 2 major VOC sources (He et al., 2002; Hui et al., 2018; Hui et al., 2019; Mo et al., 2017; Song et al., 2018; An et al., 2014; Mozaffar & Zhang, 2020). Whereas vehicle-related sources are more dominant in the North China Plain (NCP), Central China (CC), and Pearl River Delta region (PRD), industry-related sources are more influential in the Yangtze River Delta (YRD) area (Zhang et al., 2017; Meng et al., 2015; Sun et al., 2019; He et al., 2019; Zhang et al., 2018; An et al., 2017; Mozaffar & Zhang, 2020; Shao et al., 2016). Alkanes, Alkenes, aromatics, oxygenated-VOCs (OVOCs), and halocarbons are the most common VOC-groups in the atmosphere (Hui et al., 2019; Hung-Lung et al., 2007; Song et al., 2018; Tiwari et al., 2010; He et al., 2019; Na et al., 2001; Hui et al., 2018). VOC concentration and composition changes depending on seasons, for example, the contribution from biogenic and solvent utilization increases in summer, and contribution from combustion sources increases in winter (Mo et al., 2017; Song et al., 2018; An et al., 2014). The chemical reactivity of VOC depends on its chemical composition, for instance, alkenes and aromatics are generally more reactive than alkanes (Carter, 2010). To understand the chemical reactivity ~~and secondary product formation ability~~ of VOCs, analysis of OH radical loss rate (L^{OH}), ~~ozone formation potential (OFP), and secondary organic aerosol potential (SOAP) are is~~ commonly used (Song et al., 2018; He et al., 2019; Hui et al., 2018); Hui et al., 2019). Industries are an important source of VOC, and different reactive and hazardous VOCs emissions from industries are already reported in different areas on earth (Zhang et al., 2018; Na et al., 2001; Hung-Lung et al., 2007; Yan et al. 2016; Tiwari et al., 2010; Shi et al., 2015; Zhang et al., 2018b). For instance, Zhang et al. (2018) reported a high concentration of alkanes (82%) and lifetime cancer risk of different aromatics and halocarbons in a petroleum refinery in Guangzhou, China. A high concentration of OVOCs (63%) was observed in an industrial area in Ulsan, Korea (Na et al., 2001). Hung-Lung et al.(2007) mentioned a high concentration of aromatics in an industrial area in Taiwan. A high concentration of halocarbons (49%) was observed in an iron smelt plant in Liaoning, China (Shi et al., 2015). Zhang et al. (2018) mentioned a high concentration of alkanes (42%) and aromatics (20%) in a petrochemical and

other industries affected area in Shanghai, China. High concentrations of aliphatic and aromatics were observed in a petrochemical industrial area in Yokohama, Japan (Tiwari et al., 2010). Therefore, VOC composition varied among the industries/industrial areas in different regions. Mostly short-term investigations were performed to characterize the VOCs in industry-affected areas. In the current study, we carried out a comprehensive investigation on VOC in an industrial area in Nanjing for about 1 month in winter, spring, and summer and 3 months in autumn between July 2018 and May 2020. Nanjing is located in the YRD region which is mainly affected by industrial emissions. Several VOC investigations have already been performed in the Nanjing industrial area but OVOCs and halocarbons were not measured in those studies (An et al., 2017; An et al., 2014). However, OVOCs and halocarbons are already mentioned as one of the highest concentrated VOC-groups in other industrial regions (Na et al., 2001; Shi et al., 2015). In the current study area, a high concentration of alkanes (45%) and alkenes (25%) were observed in a previous investigation (An et al., 2014). Besides the incomplete VOC measurements, O₃ formation sensitivity to its precursors was not investigated properly using a photochemical box model in Nanjing. Moreover, source apportionment of VOCs was not conducted for different seasons of a year.

In the current study, we report the variations in concentrations and compositions of VOC during the observation period. We present the possible source areas and potential sources of VOC based on potential source contribution function (PSCF) and positive matrix factorization (PMF) model analysis. We also present the contributions of different sources to ambient VOC during the measurement period. We report the chemical reactivity and secondary product formation capacity of the VOC using L^{OH}, OPF, and SOAP analysis. We also present the sensitivity analysis of O₃ formation using empirical kinetic modelling approach (EKMA) and relative incremental reactivity (RIR) analysis. Therefore, this study provides valuable information to the scientific community and policymakers.

2 Material and Methods

2.1 Sampling Site Description, Gases Analysis, and Meteorology Data

255 | Field measurements were carried out for about 1 month in winter, spring, and summer and 3
months in autumn from-between July 2018 ~~to~~and May 2020 at Nanjing University of
Information Science and Technology (32.1°N, 118.4°E), which is located in an industrial area in
Nanjing, China. The sampling site was on the rooftop of a building (~20 m). The sampling site
is surrounded by different chemical and petrochemical industries, steel plants, gas stations, high
traffic roads, and residential areas. A detailed description of the sampling site can be found
260 | elsewhere (Mozaffar et al., 2020).

We analysed ambient air VOCs using an online GC-FID/MS instrument (AC-GCMS 1000,
Guangzhou Hexin Instrument Co., Ltd., China). FID detector analysed C2-C5 VOCs and MS
analysed C6-C12 VOCs. The instrument analysed one sample at every hour. During the
investigation period, we inspected and calibrated the instrument regularly to ensure the accuracy
265 | of the data. We monitored the O₃ concentrations using a 49i O₃ analyser (Thermo Fisher
Scientific Inc., USA), NO, NO₂ and NO_x concentrations were measured using a 42i NO-NO₂-
NO_x analyser (Thermo Fisher Scientific Inc., USA), SO₂ concentrations were followed using a
43i SO₂ analyser (Thermo Fisher Scientific Inc., USA), and CO concentrations were measured
using a 48i CO analyser (Thermo Fisher Scientific Inc., USA). We also measured temperature
270 | and relative humidity, wind speed, wind direction, and solar radiation by HMP155 (Vaisala,
Finland), 010C (Met One Instruments, Inc., USA), 020CC (Met One Instruments, Inc., USA),
and CNR4 (Kipp & Zonen, The Netherlands) analysers, respectively. A detailed description of
the instrumentation, sampling procedure, analysis, quality control, and calibration procedure can
be found elsewhere (Mozaffar et al., 2020).

275 | 2.2 Positive Matrix Factorization (PMF) model and Potential Source Contribution Function (PSCF)

We used the positive matrix factorization (PMF) model (US Environmental Protection Agency,
USEPA, version 5.0) for the source apportionments of VOCs. A detailed description of the
model can be found elsewhere (Hui et al., 2019; Song, ~~Tan, Feng, Qu, Liu,~~ et al., 2018). In this
280 | study, we used 620 potential VOC tracers (Fig. S1 - S4) in the PMF model to analyse the VOC
sources for different seasons. The error fraction was set to 20% for the sample data uncertainty

estimation. We explored the PMF factor number from 4-8 to determine the optimal number of sources. Finally, we decided to choose an 7 to 8-factor solution ($Q_{\text{true}}/Q_{\text{robust}} = \sim 1.0$) for different seasons.

285 We used the potential source contribution function (PSCF) to locate possible source areas of VOCs for different seasons during the investigation period. We used Zefir analysis software to do the PSCF analysis and the Hysplit4 model to cluster the backward trajectories (Petit et al., 2017). Backward trajectories in the sampling site were estimated using the data provided by the National Centers for Environmental Prediction (<ftp://arlftp.arlhq.noaa.gov/pub/archives/gdas1>).
290 We estimated ~~24-72~~ hr backward trajectories 24 times a day arriving at 500 m above the ground surface using the hysplit4 model. For the PSCF analysis, we divided the geographic region covered by the back trajectories into an array of $0.1^\circ \times 0.1^\circ$ grid cells and used the mean TVOCs concentration as the VOC reference value. More details about the PSCF analysis can be found in previous studies (Chen et al., 2018).

295

2.3 OH radical loss rate (L^{OH}), ~~Ozone formation potential (OFP), and Secondary organic aerosol potential (SOAP)~~

To evaluate the daytime photochemistry of VOCs, we estimated their OH radical loss rate (L^{OH}). The following equation was used to estimate the L^{OH} (s^{-1}) (Zhang et al., 2020).

300
$$L^{\text{OH}} = [\text{VOC}]_i \times K_i^{\text{OH}} \quad (1)$$

Where $[\text{VOC}]_i$ is the concentration of VOC species i (molecule cm^{-3}), K_i^{OH} ($\text{cm}^3 \text{ molecule}^{-1} \text{ s}^{-1}$) is the reaction rate constant of i VOC with OH radical. The K^{OH} values for the VOCs are collected from Carter (2010) (Table S1).

305 ~~The Ozone formation potential (OFP) of the VOCs is their maximum contribution to the O_3 formation (Hui et al., 2018a). The OFP (ppbv) of the VOCs was estimated using the following equation:~~

~~$$\text{OFP} = [\text{VOC}]_i \times \text{MIR}_i$$~~
~~(2)~~

310 ~~Where MIR_i is the maximum incremental reactivity of the i VOC. The MIR values for the VOCs are also collected from Carter (2010) (Table S1).~~

~~The contribution of VOCs to the formation of secondary organic aerosol is estimated by secondary organic aerosol potential (SOAP) (Song et al., 2018). We estimated the SOAP (ppbv) of VOCs using the following equation.~~

$$SOAP = [VOC]_i \times SOAP_i^P$$

(3)

~~Where $SOAP_i^P$ is the SOA formation potential of the i VOC on a mass basis relative to toluene (Derwent et al., 2010). In this study, the $SOAP^P$ factors of the VOCs are collected from Derwent et al. (2010) (Table S1).~~

2.4 Empirical Kinetic Modelling Approach (EKMA) and Relative Incremental Reactivity (RIR)

The empirical kinetic modelling approach (EKMA) is a well-known procedure to develop the O₃ formation reduction strategy by testing the relationship between ambient O₃ and its precursors (He et al., 2019; Hui et al., 2018; Vermeuel et al., 2019; Tan et al., 2018). In this study, we used the Framework for 0-D Atmospheric Model (FOAM v 3.2, Wolfe et al., 2016), a photochemical box model run by Master Chemical Mechanism (MCM) v3.2 chemistry (Jenkin et al., 1997; 2003, 2015; Saunders et al., 2003), to get the data for the EKMA isopleth. The FOAM-MCM box model can simulate 16940 reactions of 5733 chemical species. The box model was run using the VOCs and gas concentrations and the meteorological data as input. To generate the O₃ isopleth from the model simulated data, a total of 121 reduction scenarios (11 NO_x × 11 VOC) were simulated and the maximum O₃ produced in each scenario was saved.

The O₃ formation sensitivity to its precursors' concentrations can also be assessed by the relative incremental reactivity (RIR, Cardelino & Chameides, 1995). We also utilized the FOAM-MCM box model data to estimate the RIR. The RIR is simply defined as the percentage change in O₃ formation per percentage change in precursor's concentration. In this study, we reduced the precursor's concentration by 10% for the RIR estimation. The RIR was estimated using the following equation.

$$RIR(X) = \frac{[P_{O_3}(X) - P_{O_3}(X - \Delta X)] / P_{O_3}(X)}{[\Delta X] / [X]}$$

(4)

Where $[X]$ is the observed concentration of a precursor X , $[\Delta X]$ is the changes in the concentration of X . $P_{O_3}(X)$ and $P_{O_3}(X - \Delta X)$ are the simulated net O_3 production with the observed and the reduced concentration of the precursor X , respectively.

3 Results and discussion

3.1 Overview of the metrological conditions and air pollutants concentrations

The time series of the hourly inorganic air pollutants, meteorological parameters, and TVOC concentrations estimated with all the measured VOCs and without halocarbons are shown in Fig. 1. The discontinuity of the time series data is due to the failure of the instruments. The measured data from July to August 2018, September to November 2018, December 2018 to January 2019, and April to May 2020 are termed as summer, autumn, winter, and springtime data, respectively. Overall, the observed temperature and solar radiation gradually decreased from summer to winter and increased back to the summertime level in spring. The temperature ranged between -5.7 and 41.4 °C during the measurement period. The relative humidity values varied from 18 to 100% and high values were generally observed in winter and autumn. During the observation period, wind speed ranged between 0.1 and 7.5 ms^{-1} . Wind prevailed at the sampling site from many directions during the measurement periods; more details about the wind direction will be discussed in Sect.3.3.2. The O_3 and NO_x concentrations varied from 2 to 160 ppbv and 0.4 to 90 ppbv, respectively. Whereas high O_3 concentrations (>80 ppbv) were observed in summer and spring, high NO_x concentrations were measured in winter and at the end of autumn. The CO and SO_2 concentrations ranged from 83 to 3398 ppbv and 0.5 to 21 ppbv, respectively. Generally, high concentrations of CO and SO_2 were observed in winter and spring. The measured NO and NO_2 concentrations varied from 0.4 to 51 ppbv and 1 to 79 ppbv, respectively. In general, the high NO and NO_2 concentrations were observed in autumn and winter. The TVOCs concentrations estimated with all the measured VOCs varied between 9 and 393 ppbv during the observation period and the high values were measured in autumn and winter. More details about the abovementioned parameters will be discussed in the following section.

3.2 Concentration and composition of VOCs

In total 100 VOCs were observed in Nanjing industrial area, including 27 alkanes, 11 alkenes, 1 alkyne, 17 aromatics, 31 halocarbons, 12 OVOCs, and 1 other (carbon disulfide) (Table S2).

370 Ethane (5.8 ± 2.5 ppbv), propane (4.2 ± 1.5 ppbv), and ethylene (3 ± 1.6 ppbv) were the most abundant VOCs in the study area during the observation period. However, we observed season-wise variations in the order of abundant VOC species (Table S2). For instance, acetone was the 3rd highest concentrated VOC in spring. The abovementioned 4 VOC species are also frequently mentioned as the most abundant VOCs in different regions in China (Deng et al., 2019; He et al., 375 2019; J. Li et al., 2018; Ma et al., 2019). We compared the individual VOC concentrations with the available data presented in recent investigations. The individual VOC concentrations in the current observation were similar to those in the previous investigations in the same study area, however, they were almost twice of those found in a nonindustrial suburban area in Nanjing (Table S2). Some of the differences in comparison to the study performed in the nonindustrial suburban area in Nanjing (Wu et al., 2020) may be due to the differences in the observation period. The yearly concentrations reported in the study performed in the nonindustrial suburban area in Nanjing were probably estimated over continuous measurement data for a year. However, the yearly concentrations in the current observation were estimated using the data which were not continuously measured during all the days of a year. The autumntime individual VOC concentrations in the current observation were about 1.4 fold lower than those measured in Beijing during October-November (Li et al., 2015). The winter time individual VOC concentrations in the current observation were also about 1.4 fold lower than those measured in and Shanghai during November-January (Zhang et al., 2018), ~~but~~ But, the yearly individual VOC concentrations in the current observation were similar to those measured in Guangzhou during 380 June-May (Zou et al., 2015). During the observation period, the concentrations of different VOC-groups were in the order of alkanes (21 ± 7 ppbv, 35%)> halocarbons (14.3 ± 7.3 ppbv, 24%)> aromatics (9.9 ± 5.8 ppbv, 17%)> OVOCs (7.5 ± 1.9 ppbv, 13%)> alkenes (5 ± 1.9 ppbv, 8%)> alkynes (1.4 ± 0.3 ppbv, 2%)> others (0.5 ± 0.2 ppbv, 1%). However, we noticed relatively higher proportions of OVOCs (14% and 18%) than the aromatics (12% and 14%) in summer and spring (Fig. 2c & f). The relatively higher contribution of OVOCs in summer and spring 385 could be related to the biogenic emissions (e.g. acetone, MEK from trees). Indeed, the relative contribution of acetone and MEK to the TVOCs were higher in summer and spring than those in autumn and winter (Table S2). Huang et al. (2019) reported that the industries, biogenic emissions, and secondary formation are the main source of OVOCs in southern China. Relatively 390 high proportions of ~~heal~~ hydrocarbons and aromatics were observed in autumn (25.7 and 19.3%, 395

respectively) and winter (25.8 and 17.6%, respectively) compared to those measured in summer (20.4 and 11.8%, respectively) and spring (20.3 and 13.6%, respectively) (Fig. 2f). The high proportions of ~~halo~~hydrocarbons and aromatics in autumn and winter could be related to the burning of biomass and fossil fuel for additional heating. Similar to the observation in the current study, the alkane is generally the most abundant VOC group in China (Mozaffar & Zhang, 2020). The relatively high contribution from halocarbons to the TVOCs could be related to the industrial emissions in the study area. In previous studies in an iron smelt plant in Liaoning, China, a high concentration of halocarbons (49%) was observed (Shi et al., 2015). However, halocarbons and OVOCs were not measured in previous investigations in the same study area (An et al., 2014; An et al., 2017; Shao et al., 2016) and also in another suburban area in Nanjing (Wu et al., 2020). Either aromatics or alkenes was mentioned as the second most abundant VOC-group in those studies in Nanjing, which is the 3rd and 5th most abundant VOC group in the current investigation. In Shanghai, a nearby city, alkanes (42%) and alkenes (26%) were two major VOC-groups and halocarbons and OVOCs were not reported (Zhang et al., 2018). The TVOCs concentration including halocarbons was 59.8±28.6 ppbv over the whole observation period, and relatively higher TVOCs concentrations were measured in autumn (83±20 ppbv) and winter (77.5±16.8 ppbv) compared to those in spring (39.6±13.1 ppbv) and summer (38.8±10.2 ppbv). The TVOCs concentration without halocarbons were 45.4±20.4, 61.7±14.6, 57.4±11.8, 31.6±10.9, and 30.9±8.2 ppbv during the whole observation period, autumn, winter, spring and summer, respectively. About 1.5 times higher TVOCs concentration was observed relative to the previous investigation in the same study area (An et al., 2014; An et al., 2017). Besides, we also found 3 times higher TVOCs concentration compared to the one in a nonindustrial suburban area in Nanjing (Wu et al., 2020). As mentioned before, Hhalocarbons and OVOCs were not measured-reported in the previous investigation in the same study area (An et al., 2014; An et al., 2017) and in a nonindustrial suburban area in Nanjing (Wu et al., 2020). The current TVOCs concentration without halocarbons and OVOCs was similar to the previous investigation in the same study area, however, 2 folds higher than the one reported in the nonindustrial suburban area in Nanjing-those previous studies in Nanjing, it could be one of the reasons for the relatively high TVOCs concentration in the current study. Observed autumn-time and wintertime TVOCs concentrations including halocarbons were was similar to ~~those the one~~ measured in urban Beijing (86.2 ppbv ~~in autumn~~ during 17-31 October) (Li et al., 2015). and Wintertime TVOCs

435 ~~concentrations without OVOCs in Shanghai (94.1 ppbv during in winter Nov-Jan) was higher than~~
~~the current observation (70±15.1 ppbv) (Li et al., 2015; (Zhang et al., 2018). Similarly,~~
~~Observed summertime TVOCs concentration was similar to those found in urban Xi'an (42.6~~
440 ~~ppbv, estimation includes halocarbons and OVOCs), Wuhan (43.9 ppbv estimation includes~~
~~halocarbons and OVOCs) (Zeng et al., 2018; Sun et al., 2019). Yearly TVOCs concentration~~
~~including halocarbons and OVOCs was 1.7 folds higher than the one found in Wuhan (Hui et~~
~~al., 2018b). Besides, yearly TVOCs concentration without halocarbons and OVOCs (37.9 ppbv)~~
~~was similar to Lanzhou, Chengdu, and Tokyo, however, 1.5 times higher than those reported for~~
445 ~~Tianjin and Ningbo (Jia et al., 2016;(Hui et al., 2018b; B. Liu et al., 2016a; Hoshi et al., 2008;~~
~~Mo et al., 2017; Song et al., 2018). However, yearly TVOCs concentration was 1.5-3 folds~~
~~higher than those in Lanzhou, Wuhan, Tianjin, Ningbo, Chengdu, London, Los Angeles, and~~
~~Tokyo (Jia et al., 2016; Hui et al., 2018; B. Liu et al., 2016a; Mo et al., 2017; Song et al., 2018;~~
~~von Schneidmesser et al., 2010; Warneke et al., 2012; Hoshi et al., 2008). The diurnal variation~~
450 ~~of the TVOCs, alkenes, aromatics, halocarbons, OVOCs, and alkanes concentrations showed a~~
~~double-hump structure (Fig. 2a, b, d, & e). This double-hump pattern indicates the contribution~~
~~of traffic emission during the rush-hours in the morning and evening. The lowest concentration~~
~~of the TVOCs and different VOC-groups reached 12:00-16:00. Oppositely, the highest~~
~~concentration of O₃ reached at that period (Fig. 3). The lowest O₃ concentrations were observed~~
455 ~~in winter which was consistent with the solar radiations.~~

3.3 Sources of VOCs

3.3.1 Specific Ratios

455 ~~The use of the toluene/benzene (T/B) ratio is one of the simplest ways to preliminary analyse the~~
~~VOC sources. If the T/B ratio is < 2, the study area is mainly affected by vehicle emissions (Hui~~
~~et al., 2018, 2019). If the T/B ratio is > 2, the study area is influenced by other sources (e.g.~~
~~industry, solvent utilization) beside vehicle emissions (Kumar et al., 2018; Niu et al., 2012; Li et~~
~~al., 2019). Moreover, the T/B ratios are ranged between 0.2-0.6 in coal and biomass burning~~
~~affected areas (Wang et al., 2009; Akagi et al., 2011). The diurnal variations in T/B ratios during~~
~~different seasons are depicted in Fig. 4 (a, b, c, & d). The mean values of T/B ratios were ranged~~
460 ~~between 0.9-2 (1.4±0.3), 1.3-2 (1.7±0.2), 1.1-1.6 (1.4±0.1), and 1.4-2.7 (1.9±0.3) during~~
~~summer, autumn, winter, and spring, respectively. As the mean values of T/B ratios were around~~

2, the study area could be mainly affected by vehicle emissions. The double-hump pattern in the diurnal variations in T/B ratios also indicates that the rush-hour traffic had a significant influence on the VOCs concentrations in the study area. Besides, the 75th percentiles of T/B ratios were above 2 most of the investigation periods, therefore, the study area could also be influenced by industrial emissions.

Figure 4 (e, f, g, & h) shows the ratios of different alkanes and aromatics to acetylene. Acetylene is a tracer of combustion sources, the ratios of different alkanes and aromatics to acetylene are used to comprehend the contribution of other sources to combustion sources. The mean ratios of propane, n-butane, and i-butane to acetylene were around 2.0-4.0, 0.7-1.6, and 0.4-0.8, respectively during all the seasons, which were smaller than those (11.5, 1.8, and 2.6, respectively) observed in Guangzhou city centre, which was affected by liquefied petroleum gas (LPG) emissions (Zhang et al., 2013). Therefore, LPG usages probably contributed a little fraction to the alkanes in the study area. The mean ratios of benzene, toluene, C8-aromatics, and C9-aromatics to acetylene were around 0.3-1.0, 0.4-1.1, 0.2-0.6, and 0.1, respectively during all the seasons. The observed ratios of benzene and toluene to acetylene were much higher than those found in Jianfeng Mountains in Hainan (0.2 and 0.1, respectively) but comparable to those measured in urban Guangzhou (0.4 and 0.4-1, respectively) (Tang et al., 2007). Besides, the observed ratios of C8-aromatics and C9-aromatics to acetylene were comparable to traffic emission influenced urban Guangzhou (0.68 and 0.2, respectively) and Wuhan (0.5 and 0.2, respectively) (Zhang et al., 2013; Hui et al., 2018). Therefore, vehicle exhaust probably contributed significantly to the aromatics in the study area.

3.3.2 Potential Source Contribution Function (PSCF)

Besides the local sources, both the long and short distance transport of air mass could bring VOCs to the study area. Figure 5 shows the wind cluster and PSCF analysis results for different seasons. During summer, the major air masses were was short-distance transports from the southwest (4044%) direction and two long distance transports from southeast (3931 and 25%) directions. A minor air mass (21%) was transported from the east direction. High PSCF values were in the nearby southwest, and southeast, and east directions; therefore, VOC pollution in the study area was mainly affected by the short-distance transport from the south and southeast directions. During autumn, the dominant air masses were short-distance transport from the

~~northeast-northwest (5935%) and long distance transport from the northwest (3034%) directions.~~ However, according to the PSCF analysis, VOC pollution was mainly influenced by the short distance transport from the south ~~and east~~ directions. During winter, short-distance transports from the ~~northeast (46%) and~~ northwest (~~3752%~~) directions ~~were was~~ the major incoming air masses to the study area. According to the PSCF values, the short-distance air masses from the south and ~~east-north~~ directions were mainly transported VOC to the receptor site. During spring, air mass was mainly transported from the ~~southwestern-north (4950%) and eastern-southwest (3032%) directions.~~ A minor long distance air mass transported from the northwest (18%) direction. Atmospheric VOCs to the study area were mainly transported by these ~~two~~ air masses mostly from the nearby areas. Overall, the high PSCF values were concentrated around the measurement site, therefore, short distance transports from the surrounding areas and cities were the main reason for the high VOC concentration. The above conclusion perfectly makes sense as the sampling site is surrounded by different chemical and petrochemical industries, steel plants, gas stations, high traffic roads, and residential areas.

3.3.3 PMF Model Analysis

~~Differences were observed among the source profiles of VOCs obtained for different seasons (Sect. S1). For instance, the biogenic source was identified in summer, biomass burning source was distinguished in autumn, and LPG/NG usage source was found in winter and spring. However, industry and vehicle-related VOC sources were identified during all the measurement seasons. According to PMF model results, aromatics were emitted from solvent usages, vehicle, and industry related sources. Besides, industry and combustion processes were the main sources of halocarbons and OVOCs. Moreover, alkanes and alkenes were emitted from vehicle exhaust and fuel usage sources.~~

~~Figure 6 shows the relative contributions of different sources to ambient VOCs during different seasons. Overall, industry-related sources contributed to the major portion of the ambient VOC concentrations followed by vehicle emission. Industrial emission accounted for about 32%, 47%, 45%, and 23% in summer, autumn, winter, and spring, respectively. The contributions of vehicle emission were about 34%, 26%, 24%, and 27% in summer, autumn, winter, and spring, respectively. The contribution of vehicle emission remained similar during the 4 seasons,~~

525 however, the contribution of the industrial emission increased in autumn and winter. Previous investigations performed in Beijing, Tianjin, Wuhan, Chengdu, and Shuo Zhou also found that the industry and vehicle are the two most important VOC sources (Zhang et al. 2017; Liu et al. 2016; Hui et al. 2018; Song et al. 2018) Jia et al., 2016). Besides these two sources, solvent usage (11%, 10%, 10%, and 4%, respectively) and gasoline evaporation (17%, 10%, NA, 6%, respectively) were two important VOC sources during those 4 seasons. Moreover, source contribution from the biogenic source in summer (7%), biomass burning in autumn (7%), LPG/NG usage in winter (11%) and spring (18%), and multiple sources in winter (10%) and spring (23%) was observed.

530 According to the PMF model analysis, five VOC sources were common during all the measurement seasons. They were biomass/biofuel burning, LPG/NG usage, gasoline evaporation, gasoline vehicle exhaust, and paint solvent usage (Sect. S1). The biogenic source was distinguished only in summer. Figure 6 shows the relative contributions of different sources to ambient VOCs during different seasons. Overall, vehicle-related sources contributed to the major portion of the ambient VOC concentrations. The total contributions of vehicle-related emission were about 39%, 33%, 48%, and 42% in summer, autumn, winter, and spring, respectively. The contributions of biomass/biofuel burning were about 19%, 21%, 17%, and 16.4% in summer, autumn, winter, and spring, respectively. Besides these two sources, LPG/NG usage (18%, 21%, 16%, and 18%, respectively) and paint solvent usage (8%, 12%, 11%, 5%, respectively) were two important VOC sources during those 4 seasons.

3.4 Chemical reactivity (L^{OH}) and contribution to O_3 - and SOA formation

545 The estimated loss rates of OH radical (L^{OH}) with VOCs were about 2-fold high in autumn ($13.7 s^{-1}$) and winter ($13.5 s^{-1}$) compared to those in summer ($7 s^{-1}$) and spring ($7.5 s^{-1}$) (Fig. 7 a). The relatively high L^{OH} values in autumn and winter were due to the relatively high VOC concentrations in those seasons (Fig.2). The average L^{OH} value was $10.4 \pm 3.6 s^{-1}$ over the four seasons. It was in a similar range with the values determined in Guangzhou ($10.9 s^{-1}$), Chongqing ($10 s^{-1}$), Xian ($1.6-16.2 s^{-1}$), and Tokyo ($7.7-13.4 s^{-1}$), however, higher than the values estimated in Shanghai ($2.9-5 s^{-1}$, $6.2 s^{-1}$) and Beijing ($7 s^{-1}$) (Tan et al., 2019; Zhu et al., 2019; Yoshino et al., 2012; Song et al., 2020). While alkene was the highest contributor to the L^{OH} in summer ($3 s^{-1}$, 43%) and spring ($2.6 s^{-1}$, 35%), aromatic was the maximum contributor in autumn ($6.9 s^{-1}$,

50%) and winter (5.9 s^{-1} , 44%) (Fig. 11 a & d). An increase in the OH loss rate by OVOCs was observed in spring (17%) compared to the other seasons (10, 8, and 9% in summer, autumn, and winter, respectively). Over the four seasons, the contribution of VOC-groups to L^{OH} exhibited the following trend: aromatics > alkenes > alkanes > OVOCs > halocarbons. Similar to the current study, aromatic is also mentioned as the maximum contributors to L^{OH} in different regions in China, however, the alkene is generally reported as the top contributor to L^{OH} (Zhang et al., 2020; Zhao et al., 2020; Hui et al., 2018; Song et al., 2020). Figure 7 also shows the top 10 VOCs contributing to L^{OH} for different seasons. Whereas isoprene was the highest contributor to L^{OH} in summer, styrene was the largest contributor in autumn and winter. On the other hand, naphthalene was the main contributor to L^{OH} in spring. Overall, styrene, naphthalene, ethylene, and isoprene were the main contributor to L^{OH} in the study area. In previous studies in China, these compounds are also mentioned as one of the highest contributors to L^{OH} (Zhao et al., 2020; Hui et al., 2018; Song et al., 2020).

~~The estimated O_3 -formation potential (OFP) of VOCs were about 2-times high in autumn (170.8 ppbv) and winter (175.4 ppbv) relative to those in summer (86.2 ppbv) and spring (82.8 ppbv) (Fig. 8 a). The average OFP value was 128.8 ± 51.2 ppbv during the measurement period. The springtime OFP was similar to the one estimated in Beijing (80 ppbv) (Li et al., 2015). The summertime OFP was about 1.5 times higher than the one in Xi'an (Song et al., 2020), but, about 1.4-2 folds lower than those found in Shanghai (Liu et al., 2019). The average OFP was about 1.5 times higher than the one in Wuhan (Hui et al., 2018). Whereas alkene was the major contributor to OFP in summer (37.4 ppbv, 43%), winter (72.8 ppbv, 41%), and spring (31.6 ppbv, 38%), aromatics contributed the most to OFP in autumn (62.7 ppbv, 37%) (Fig. 12 a & d). During the measurement period, the contribution of VOC groups to OFP showed the following trend: alkenes > aromatics > alkanes > OVOCs > halocarbons. The alkene is also mentioned as the top contributor to OFP in Nanjing and the same observation is commonly found in China (An et al., 2014; Hui et al., 2018; Song et al., 2018; Song et al., 2020). The top 10 VOCs contributing to OFP for different seasons are also shown in Fig. 8 (b, c, e, & f). Ethylene was the major contributor to OFP during all the season. Followed by ethylene, cis-1,3-dichloropropene was the main contributor to OFP from summer to winter. In spring, propylene was the second most contributors to OFP. Overall, different alkenes were the highest contributor to OFP in the study area. Alkenes are also mentioned as the top contributor to OFP in the previous investigations in~~

Nanjing (An et al., 2014). Therefore, the reduction of these alkenes emissions in the study area could be one of the ways to reduce ambient O₃ concentration.

The secondary organic aerosol potentials (SOAP) were about 3 times higher in autumn (1422 ppbv) and winter (1269 ppbv) than those in summer (466 ppbv) and spring (398 ppbv) (Fig. 9a). The average SOAP was 889±531 ppbv during the measurement period. The average SOAP was about 2-3 times higher than those estimated in Wuhan and Beijing (Hui et al., 2019; Li et al., 2020). Aromatics was the main contributor to SOAP during all the seasons (95-97%) (Fig. 9 a & d) which was consistent with the observations in Chengdu (Song et al., 2018), Beijing (Li et al., 2020), and Wuhan (Hui et al., 2019). During the measurement period, the contribution of VOC groups to SOAP exhibited the following trend: aromatics > alkanes > alkenes > OVOCs. Styrene, cumene, toluene, benzene, and o-xylene were the major contributor to SOAP during all the season (Fig. 9 b, c, e, & f). Therefore, the reduction of these aromatics emissions in the study area could be one of the ways to reduce ambient SOA concentration.

3.5 Sensitivity analysis of O₃ formation

Figure 10 shows the EKMA isopleth diagrams of O₃ for different seasons. In all the diagrams, VOC and NO_x = 100 % is the base case. The ridgeline divided the diagrams into two regimes, VOC-sensitive (above) and NO_x-sensitive (below) regimes. For all the seasons, the study area fell above the ridgeline. Moreover, a decrease in O₃ production was noticed with the decrease in VOC concentration. Therefore, the study area was in the VOC-sensitive regime for O₃ formation during all the seasons. As a case study, O₃ formation sensitivity to its precursors was tested on a high O₃ concentration day (July 29 2018, maximum 126 ppbv). During the high O₃ episode, the study area was also in the VOC-sensitive regime for O₃ formation (Fig. S5). We also employed the RIR analysis to evaluate the O₃ production sensitivity to VOC, NO_x, and CO concentrations (Fig. 11). The RIR value of VOC was the highest during all the seasons. It indicates that the O₃ production was more sensitive to the reduction of VOC concentration. This finding is consistent with the above results in the EKMA isopleth (Fig. 10). Except for the spring, the RIR values of CO were very small relative to those for the VOC. It indicates that the CO concentrations were relatively less important for the O₃ formation during those seasons. The RIR values for NO_x were negative during all the seasons, implying that the O₃ formation was in the NO_x-titration regime in the study area. From the above analysis, it is evident that a reduction of VOC

concentration in the study area will be the most efficient way to reduce the O₃ formation. The previous two studies performed in Nanjing also concluded the same finding based on VOC/NO_x ratios and RIR analysis (An et al., 2015; Xu et al., 2017). Our findings are also consistent with the previous studies performed in other regions in China (Tan et al., 2018a; He et al., 2019; Feng et al., 2019; Ma et al., 2019). However, NO_x-sensitive regions for O₃ formation are also found in China (Tan et al., 2018; Jia et al., 2016).

4 Conclusions

620 Industries are an important anthropogenic source of VOCs. VOC plays a major role in tropospheric chemistry and air quality. Nanjing is one of the biggest industrial cities in China. We performed a long term investigation of ambient VOCs in an industrial area in Nanjing. ~~About 1.5~~ Similar and ~~32~~-folds high TVOCs concentrations were observed compared to those previously reported in the same study area and a nonindustrial suburban area in Nanjing, respectively. ~~The relatively high TVOCs was due to halocarbons and OVOCs concentrations were not measured in those previous studies in Nanjing. Therefore, halocarbons and OVOCs were an important part of the TVOCs in Nanjing, and industrial emissions had a large influence on VOC concentration in the study area.~~ Observed TVOCs concentration was also ~~about 1.5 similar~~ ~~3-1.7~~ folds higher than those reported in other cities in China and the world, but, ~~similar 1.3 times smaller to than those the one~~ measured in urban ~~Beijing and~~ Shanghai. ~~This~~ The high VOC concentration in the study area needs to be reduced to decrease O₃ concentration and improve the local air quality. TVOCs concentrations were about 2-times high in autumn and winter compared to those in summer and spring. Generally, haze pollutions frequently happen in autumn and winter, therefore, VOC concentration reduction in these seasons is an important step to reduce haze pollutions in the study area. After alkane, halocarbon was the 2nd largest contributor to the TVOCs, indicating a high influence of industrial emissions. Generally, alkenes/aromatics/OVOCs are the 2nd largest contributor to the TVOCs in China, therefore, industries in Nanjing emitted a high amount of halocarbons into the atmosphere. As halocarbons are carcinogenic, their emissions should be reduced. PSCF analysis indicated that the short distance transports from the surrounding areas and cities were the main reason for high VOC concentration in the study area. Hence, local emissions should be reduced to decrease the haze and O₃ pollution in the study area. ~~Industries~~ Vehicle-related emissions were the major VOC

sources in the study area ~~followed by vehicles~~, thus, emission reduction from these ~~two~~-sources should get more priority. Aromatics and alkenes accounted for most of the L^{OH} , ~~OFP, and SOAP~~, thus, these 2 kinds of VOCs should get more priority in emission reduction policies and strategies. During all the seasons, the study area was in the VOC-sensitive regime for O_3 formation. Therefore, VOCs especially aromatics and alkenes emission reduction is the most effective way to decrease the local O_3 formation.

650 **Data availability**

All the data presented in this article can be accessed through <https://osf.io/bm6cs/>.

Author contribution

YLZ designed and supervised the project; MYF, FX, YCL, FC, and AM conducted the measurements; AM analysed the data and prepared the manuscript. All authors contributed in discussion to improve the article.

Competing interests

The authors declare that they have no conflict of interest.

660

Acknowledgements

The authors thank funding support from the National Nature Science Foundation of China (No. 41977305 and 41761144056), the Provincial Natural Science Foundation of Jiangsu (No. BK20180040), and the Jiangsu Innovation & Entrepreneurship Team. We are also grateful to Zijin Zhang and Meng-Yao Cao for their help on sampling.

References

- An, J., Wang, J., Zhang, Y., & Zhu, B. (2017). Source Apportionment of Volatile Organic Compounds in an Urban Environment at the Yangtze River Delta, China. *Archives of Environmental Contamination and Toxicology*, 72(3), 335–348. <https://doi.org/10.1007/s00244-017-0371-3>
- An, J., Zhu, B., Wang, H., Li, Y., Lin, X., & Yang, H. (2014a). Characteristics and source apportionment of VOCs measured in an industrial area of Nanjing, Yangtze River Delta,

- China. *Atmospheric Environment*, 97, 206–214.
<https://doi.org/10.1016/j.atmosenv.2014.08.021>
- 675 An, J., Zhu, B., Wang, H., Li, Y., Lin, X., & Yang, H. (2014b). Characteristics and source apportionment of VOCs measured in an industrial area of Nanjing, Yangtze River Delta, China. *Atmospheric Environment*, 97, 206–214.
<https://doi.org/https://doi.org/10.1016/j.atmosenv.2014.08.021>
- 680 An, J., Zou, J., Wang, J., Lin, X., & Zhu, B. (2015). Differences in ozone photochemical characteristics between the megacity Nanjing and its suburban surroundings, Yangtze River Delta, China. *Environmental Science and Pollution Research*, 22(24), 19607–19617.
<https://doi.org/10.1007/s11356-015-5177-0>
- Cardelino, C. A., & Chameides, W. L. (1995). An observation-based model for analyzing ozone precursor relationships in the urban atmosphere. *Journal of the Air and Waste Management Association*, 45(3), 161–180. <https://doi.org/10.1080/10473289.1995.10467356>
- 685 Carter, W. P. L. (2010). Development of the SAPRC-07 chemical mechanism. *Atmospheric Environment*, 44(40), 5324–5335. <https://doi.org/10.1016/j.atmosenv.2010.01.026>
- Chen, Y., Ge, X., Chen, H., Xie, X., Chen, Y., Wang, J., ... Chen, M. (2018). Seasonal light absorption properties of water-soluble brown carbon in atmospheric fine particles in Nanjing, China. *Atmospheric Environment*, 187(June), 230–240.
<https://doi.org/10.1016/j.atmosenv.2018.06.002>
- 690 Deng, Y., Li, J., Li, Y., Wu, R., & Xie, S. (2019). Characteristics of volatile organic compounds, NO₂, and effects on ozone formation at a site with high ozone level in Chengdu. *Journal of Environmental Sciences (China)*, 75(2), 334–345. <https://doi.org/10.1016/j.jes.2018.05.004>
- 695 Feng, R., Wang, Q., Huang, C. chen, Liang, J., Luo, K., Fan, J. ren, & Zheng, H. jun. (2019). Ethylene, xylene, toluene and hexane are major contributors of atmospheric ozone in Hangzhou, China, prior to the 2022 Asian Games. *Environmental Chemistry Letters*, 17(2), 1151–1160. <https://doi.org/10.1007/s10311-018-00846-w>
- Feng, T., Bei, N., Huang, R. J., Cao, J., Zhang, Q., Zhou, W., ... Li, G. (2016). Summertime ozone formation in Xi'an and surrounding areas, China. *Atmospheric Chemistry and Physics*, 16(7), 4323–4342. <https://doi.org/10.5194/acp-16-4323-2016>
- 700 He, Z., Wang, X., Ling, Z., Zhao, J., Guo, H., Shao, M., & Wang, Z. (2019). Contributions of different anthropogenic volatile organic compound sources to ozone formation at a receptor

- 705 site in the Pearl River Delta region and its policy implications. *Atmospheric Chemistry and Physics*, 19(13), 8801–8816. <https://doi.org/10.5194/acp-19-8801-2019>
- Huang, X., Wang, C., Zhu, B., Lin, L., & He, L. (2019). Exploration of sources of OVOCs in various atmospheres in southern. *Environmental Pollution*, 249, 831–842. <https://doi.org/10.1016/j.envpol.2019.03.106>
- Hui, L., Liu, X., Tan, Q., Feng, M., An, J., Qu, Y., ... Cheng, N. (2019). VOC characteristics, sources and contributions to SOA formation during haze events in Wuhan, Central China. *Science of the Total Environment*, 650, 2624–2639. <https://doi.org/10.1016/j.scitotenv.2018.10.029>
- 710 Hui, L., Liu, X., Tan, Q., Feng, M., An, J., Qu, Y., ... Jiang, M. (2018a). Characteristics, source apportionment and contribution of VOCs to ozone formation in Wuhan, Central China. *Atmospheric Environment*, 192(August), 55–71. <https://doi.org/10.1016/j.atmosenv.2018.08.042>
- 715 Hui, L., Liu, X., Tan, Q., Feng, M., An, J., Qu, Y., ... Jiang, M. (2018b). Characteristics, source apportionment and contribution of VOCs to ozone formation in Wuhan, Central China. *Atmospheric Environment*, 192(2), 55–71. <https://doi.org/10.1016/j.atmosenv.2018.08.042>
- 720 Hung-Lung, C., Jiun-Horng, T., Shih-Yu, C., Kuo-Hsiung, L., & Sen-Yi, M. (2007). VOC concentration profiles in an ozone non-attainment area: A case study in an urban and industrial complex metroplex in southern Taiwan. *Atmospheric Environment*, 41(9), 1848–1860. <https://doi.org/https://doi.org/10.1016/j.atmosenv.2006.10.055>
- Jenkin, M. E., Young, J. C., & Rickard, A. R. (2015). The MCM v3.3.1 degradation scheme for isoprene. *Atmospheric Chemistry and Physics*, 15(20), 11433–11459. <https://doi.org/10.5194/acp-15-11433-2015>
- 725 Jenkin, Michael E., Saunders, S. M., & Pilling, M. J. (1997). The tropospheric degradation of volatile organic compounds: A protocol for mechanism development. *Atmospheric Environment*, 31(1), 81–104. [https://doi.org/10.1016/S1352-2310\(96\)00105-7](https://doi.org/10.1016/S1352-2310(96)00105-7)
- 730 Jia, C., Mao, X., Huang, T., Liang, X., Wang, Y., Shen, Y., ... Gao, H. (2016). Non-methane hydrocarbons (NMHCs) and their contribution to ozone formation potential in a petrochemical industrialized city, Northwest China. *Atmospheric Research*, 169, 225–236. <https://doi.org/10.1016/j.atmosres.2015.10.006>
- Li, J., Xie, S. D., Zeng, L. M., Li, L. Y., Li, Y. Q., & Wu, R. R. (2015). Characterization of

- 735 ambient volatile organic compounds and their sources in Beijing, before, during, and after
Asia-Pacific Economic Cooperation China 2014. *Atmospheric Chemistry and Physics*,
15(14), 7945–7959. <https://doi.org/10.5194/acp-15-7945-2015>
- Li, Jing, Zhai, C., Yu, J., Liu, R., Li, Y., Zeng, L., & Xie, S. (2018). Spatiotemporal variations of
ambient volatile organic compounds and their sources in Chongqing, a mountainous
740 megacity in China. *Science of the Total Environment*, 627, 1442–1452.
<https://doi.org/10.1016/j.scitotenv.2018.02.010>
- Liu, B., Liang, D., Yang, J., Dai, Q., Bi, X., Feng, Y., ... Xu, H. (2016). Characterization and
source apportionment of volatile organic compounds based on 1-year of observational data
in Tianjin, China. *Environmental Pollution*, 218, 757–769.
745 <https://doi.org/10.1016/j.envpol.2016.07.072>
- Ma, Z., Liu, C., Zhang, C., Liu, P., Ye, C., Xue, C., ... Mu, Y. (2019). The levels, sources and
reactivity of volatile organic compounds in a typical urban area of Northeast China. *Journal
of Environmental Sciences*, 79, 121–134. <https://doi.org/10.1016/j.jes.2018.11.015>
- Meng, H. A. N., Xueqiang, L. U., Chunsheng, Z., Liang, R. A. N., & Suqin, H. A. N. (2015).
750 Characterization and Source Apportionment of Volatile Organic Compounds in Urban and
Suburban Tianjin, China. *Advances in Atmospheric Sciences*, 32(3), 439–444.
<https://doi.org/10.1007/s00376-014-4077-4.1>
- Mo, Z., Shao, M., Lu, S., Niu, H., Zhou, M., & Sun, J. (2017). Characterization of non-methane
hydrocarbons and their sources in an industrialized coastal city, Yangtze River Delta,
755 China. *Science of the Total Environment*, 593–594, 641–653.
<https://doi.org/10.1016/j.scitotenv.2017.03.123>
- Mozaffar, A., & Zhang, Y. L. (2020). Atmospheric Volatile Organic Compounds (VOCs) in
China: a Review. *Current Pollution Reports*, 6(3), 250–263. <https://doi.org/10.1007/s40726-020-00149-1>
- 760 Mozaffar, A., Zhang, Y. L., Fan, M., Cao, F., & Lin, Y. C. (2020). Characteristics of
summertime ambient VOCs and their contributions to O₃ and SOA formation in a suburban
area of Nanjing, China. *Atmospheric Research*, 240(February).
<https://doi.org/10.1016/j.atmosres.2020.104923>
- Na, K., Kim, Y. P., Moon, K.-C., Moon, I., & Fung, K. (2001). Concentrations of volatile
765 organic compounds in an industrial area of Korea. *Atmospheric Environment*, 35(15), 2747–

2756. [https://doi.org/https://doi.org/10.1016/S1352-2310\(00\)00313-7](https://doi.org/https://doi.org/10.1016/S1352-2310(00)00313-7)

- Petit, J. E., Favez, O., Albinet, A., & Canonaco, F. (2017). A user-friendly tool for comprehensive evaluation of the geographical origins of atmospheric pollution: Wind and trajectory analyses. *Environmental Modelling and Software*, 88, 183–187.
770 <https://doi.org/10.1016/j.envsoft.2016.11.022>
- Saunders, S. M., Jenkin, M. E., Derwent, R. G., & Pilling, M. J. (2003). Protocol for the development of the Master Chemical Mechanism, MCM v3 (Part A): Tropospheric degradation of non-aromatic volatile organic compounds. *Atmospheric Chemistry and Physics*, 3(1), 161–180. <https://doi.org/10.5194/acp-3-161-2003>
- 775 Shao, P., An, J., Xin, J., Wu, F., Wang, J., Ji, D., & Wang, Y. (2016). Source apportionment of VOCs and the contribution to photochemical ozone formation during summer in the typical industrial area in the Yangtze River Delta, China. *Atmospheric Research*, 176–177, 64–74. <https://doi.org/10.1016/j.atmosres.2016.02.015>
- 780 Shi, J., Deng, H., Bai, Z., Kong, S., Wang, X., Hao, J., ... Ning, P. (2015). Emission and profile characteristic of volatile organic compounds emitted from coke production, iron smelt, heating station and power plant in Liaoning Province, China. *Science of the Total Environment*, 515–516(x), 101–108. <https://doi.org/10.1016/j.scitotenv.2015.02.034>
- 785 Song, M., Li, X., Yang, S., Yu, X., Zhou, S., Yang, Y., ... Zhang, Y. (2020). Spatiotemporal Variation, Sources, and Secondary Transformation Potential of VOCs in Xi'an, China, 30(August). Retrieved from <https://doi.org/10.5194/acp-2020-704>
- Song, M., Tan, Q., Feng, M., Qu, Y., & Liu, X. (2018). Source Apportionment and Secondary Transformation of Atmospheric Nonmethane Hydrocarbons in Chengdu , Southwest China. *Journal of Geophysical Research Atmospheres*, 123(2), 9741–9763. <https://doi.org/10.1029/2018JD028479>
- 790 Song, M., Tan, Q., Feng, M., Qu, Y., Liu, X., An, J., & Zhang, Y. (2018). Source Apportionment and Secondary Transformation of Atmospheric Nonmethane Hydrocarbons in Chengdu, Southwest China. *Journal of Geophysical Research: Atmospheres*, 123(17), 9741–9763. <https://doi.org/10.1029/2018JD028479>
- 795 Sun, J., Shen, Z., Zhang, Y., Zhang, Z., Zhang, Q., Zhang, T., ... Li, X. (2019). Urban VOC profiles, possible sources, and its role in ozone formation for a summer campaign over Xi'an, China. *Environmental Science and Pollution Research*, 26(27), 27769–27782.

<https://doi.org/10.1007/s11356-019-05950-0>

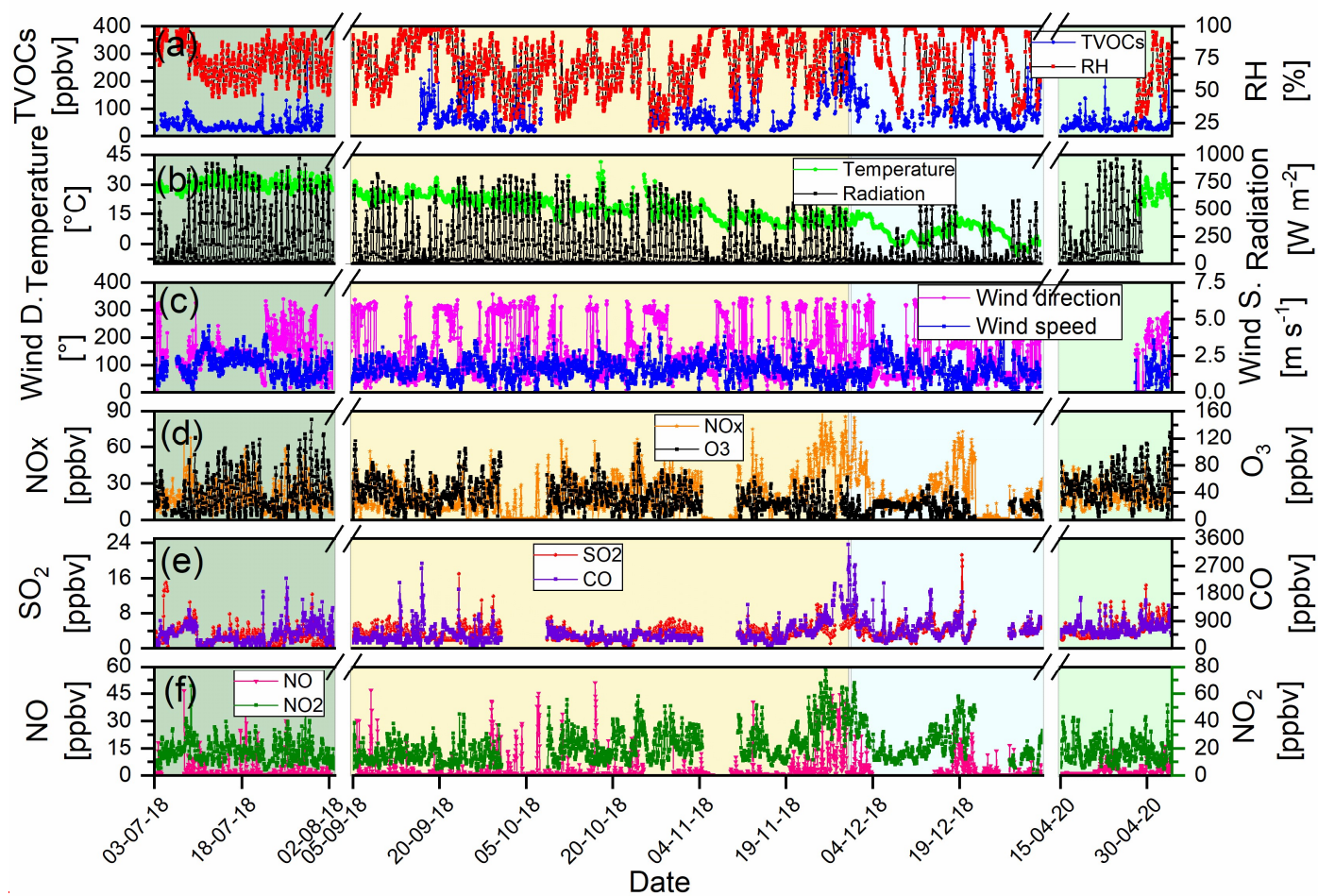
- 800 Tan, Z., Lu, K., Dong, H., Hu, M., Li, X., Liu, Y., ... Zhang, Y. (2018). Explicit diagnosis of the local ozone production rate and the ozone-NO_x-VOC sensitivities. *Science Bulletin*, 63(16), 1067–1076. <https://doi.org/10.1016/j.scib.2018.07.001>
- Tan, Z., Lu, K., Jiang, M., Su, R., Dong, H., Zeng, L., ... Zhang, Y. (2018a). Exploring ozone pollution in Chengdu, southwestern China: A case study from radical chemistry to O₃-VOC-NO_x sensitivity. *Science of The Total Environment*, 636, 775–786. <https://doi.org/10.1016/J.SCITOTENV.2018.04.286>
- 805 Tan, Z., Lu, K., Jiang, M., Su, R., Dong, H., Zeng, L., ... Zhang, Y. (2018b). Exploring ozone pollution in Chengdu, southwestern China: A case study from radical chemistry to O₃-VOC-NO_x sensitivity. *Science of the Total Environment*, 636, 775–786. <https://doi.org/10.1016/j.scitotenv.2018.04.286>
- 810 Tan, Z., Lu, K., Jiang, M., Su, R., Wang, H., Lou, S., ... Zhang, Y. (2019). Daytime atmospheric oxidation capacity in four Chinese megacities during the photochemically polluted season: A case study based on box model simulation. *Atmospheric Chemistry and Physics*, 19(6), 3493–3513. <https://doi.org/10.5194/acp-19-3493-2019>
- 815 Tiwari, V., Hanai, Y., & Masunaga, S. (2010). Ambient levels of volatile organic compounds in the vicinity of petrochemical industrial area of Yokohama, Japan. *Air Quality, Atmosphere and Health*, 3(2), 65–75. <https://doi.org/10.1007/s11869-009-0052-0>
- Vermeuel, M. P., Novak, G. A., Alwe, H. D., Hughes, D. D., Kaleel, R., Dickens, A. F., ... Bertram, T. H. (2019). Sensitivity of Ozone Production to NO_x and VOC Along the Lake Michigan Coastline. *Journal of Geophysical Research: Atmospheres*, 124(20), 10989–11006. <https://doi.org/10.1029/2019JD030842>
- 820 Wolfe, G. M., Marvin, M. R., Roberts, S. J., Travis, K. R., & Liao, J. (2016). The framework for 0-D atmospheric modeling (F0AM) v3.1. *Geoscientific Model Development*, 9(9), 3309–3319. <https://doi.org/10.5194/gmd-9-3309-2016>
- 825 Wu, R., Zhao, Y., Zhang, J., & Zhang, L. (2020). Variability and sources of ambient volatile organic compounds based on online measurements in a suburban region of nanjing, eastern China. *Aerosol and Air Quality Research*, 20(3), 606–619. <https://doi.org/10.4209/aaqr.2019.10.0517>
- Xu, Z., Huang, X., Nie, W., Chi, X., & Xu, Z. (2017). Influence of synoptic condition and

- holiday effects on VOCs and ozone production in the Yangtze River Delta region , China. *Atmospheric Environment*, 168, 112–124. <https://doi.org/10.1016/j.atmosenv.2017.08.035>
- 830 Yan, Y., Yang, C., Peng, L., Li, R., & Bai, H. (2016). Emission characteristics of volatile organic compounds from coal-, coal gangue-, and biomass-fired power plants in China. *Atmospheric Environment*, 143, 261–269. <https://doi.org/10.1016/j.atmosenv.2016.08.052>
- Yoshino, A., Nakashima, Y., Miyazaki, K., Kato, S., Suthawaree, J., Shimo, N., ... Kajii, Y. (2012). Air quality diagnosis from comprehensive observations of total OH reactivity and reactive trace species in urban central Tokyo. *Atmospheric Environment*, 49, 51–59. <https://doi.org/10.1016/j.atmosenv.2011.12.029>
- 835 Zeng, P., Lyu, X. P., Guo, H., Cheng, H. R., Jiang, F., Pan, W. Z., ... Hu, Y. Q. (2018). Causes of ozone pollution in summer in Wuhan, Central China. *Environmental Pollution*, 241(x), 852–861. <https://doi.org/10.1016/j.envpol.2018.05.042>
- 840 Zhang, F., Shang, X., Chen, H., Xie, G., Fu, Y., Wu, D., ... Chen, J. (2020). Significant impact of coal combustion on VOCs emissions in winter in a North China rural site. *Science of the Total Environment*, 720. <https://doi.org/10.1016/j.scitotenv.2020.137617>
- Zhang, H., Li, H., Zhang, Q., Zhang, Y., Zhang, W., Wang, X., ... Xia, F. (2017). Atmospheric volatile organic compounds in a typical urban area of Beijing: Pollution characterization, health risk assessment and source apportionment. *Atmosphere*, 8(3). <https://doi.org/10.3390/atmos8030061>
- 845 Zhang, Y., Li, R., Fu, H., Zhou, D., & Chen, J. (2018). Observation and analysis of atmospheric volatile organic compounds in a typical petrochemical area in Yangtze River. *Journal of Environmental Sciences*, 71, 233–248. <https://doi.org/10.1016/j.jes.2018.05.027>
- 850 Zhang, Z., Yan, X., Gao, F., Thai, P., Wang, H., Chen, D., ... Wang, B. (2018). Emission and health risk assessment of volatile organic compounds in various processes of a petroleum refinery in the Pearl River Delta ,. *Environmental Pollution*, 238, 452–461. <https://doi.org/10.1016/j.envpol.2018.03.054>
- Zhao, R., Dou, X., Zhang, N., Zhao, X., Yang, W., Han, B., ... Bai, Z. (2020). The characteristics of inorganic gases and volatile organic compounds at a remote site in the Tibetan Plateau. *Atmospheric Research*, 234(October 2019), 104740. <https://doi.org/10.1016/j.atmosres.2019.104740>
- 855 Zhu, J., Wang, S., Wang, H., Jing, S., Lou, S., Saiz-Lopez, A., & Zhou, B. (2019).

860 Observationally constrained modelling of atmospheric oxidation capacity and photochemical reactivity in Shanghai, China. *Atmospheric Chemistry and Physics Discussions*, 1–26. <https://doi.org/10.5194/acp-2019-711>

Zou, Y., Deng, X. J., Zhu, D., Gong, D. C., Wang, H., Li, F., ... Wang, B. G. (2015). Characteristics of 1 year of observational data of VOCs, NO_x and O₃ at a suburban site in Guangzhou, China. *Atmospheric Chemistry and Physics*, 15(12), 6625–6636. <https://doi.org/10.5194/acp-15-6625-2015>

870



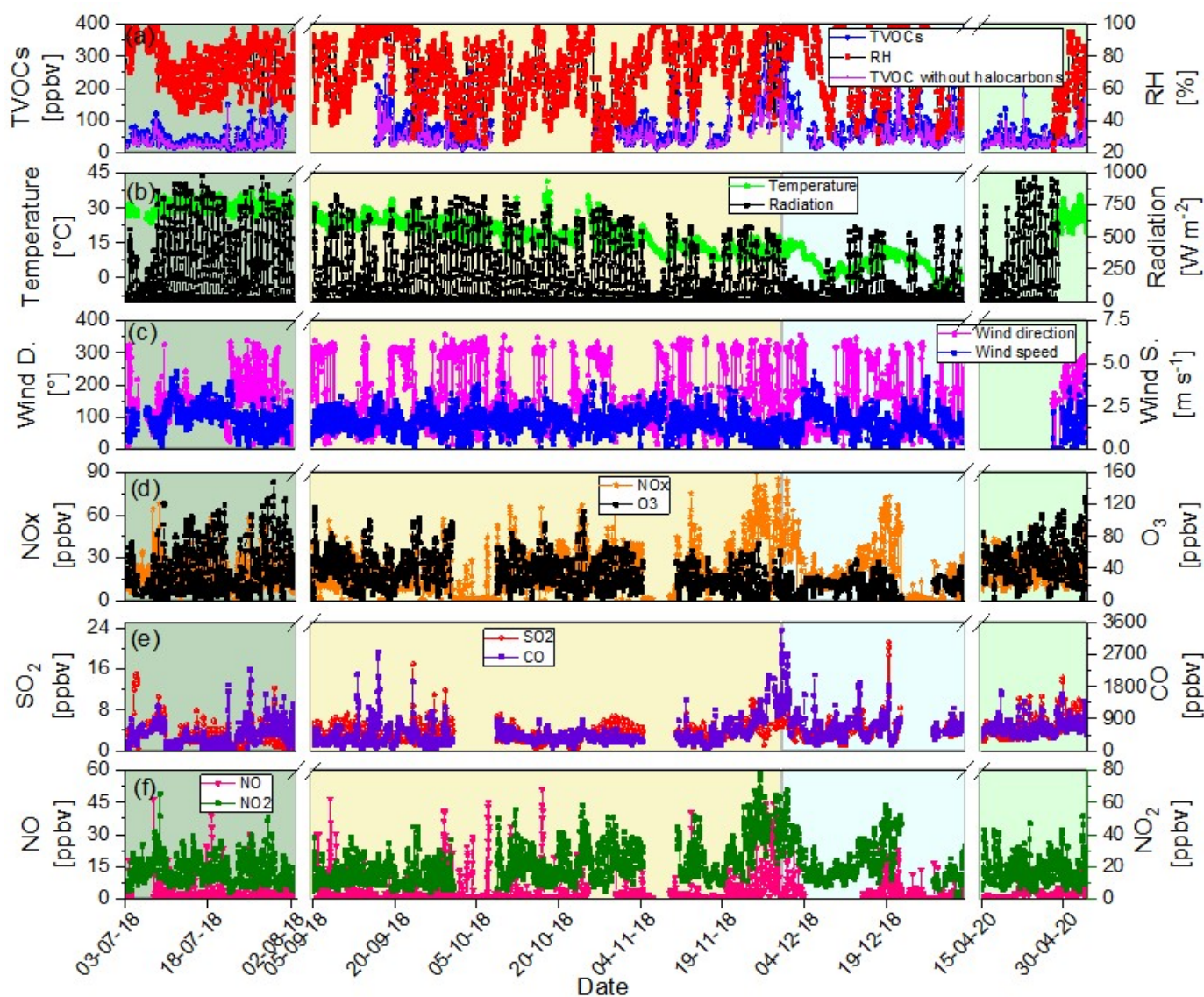
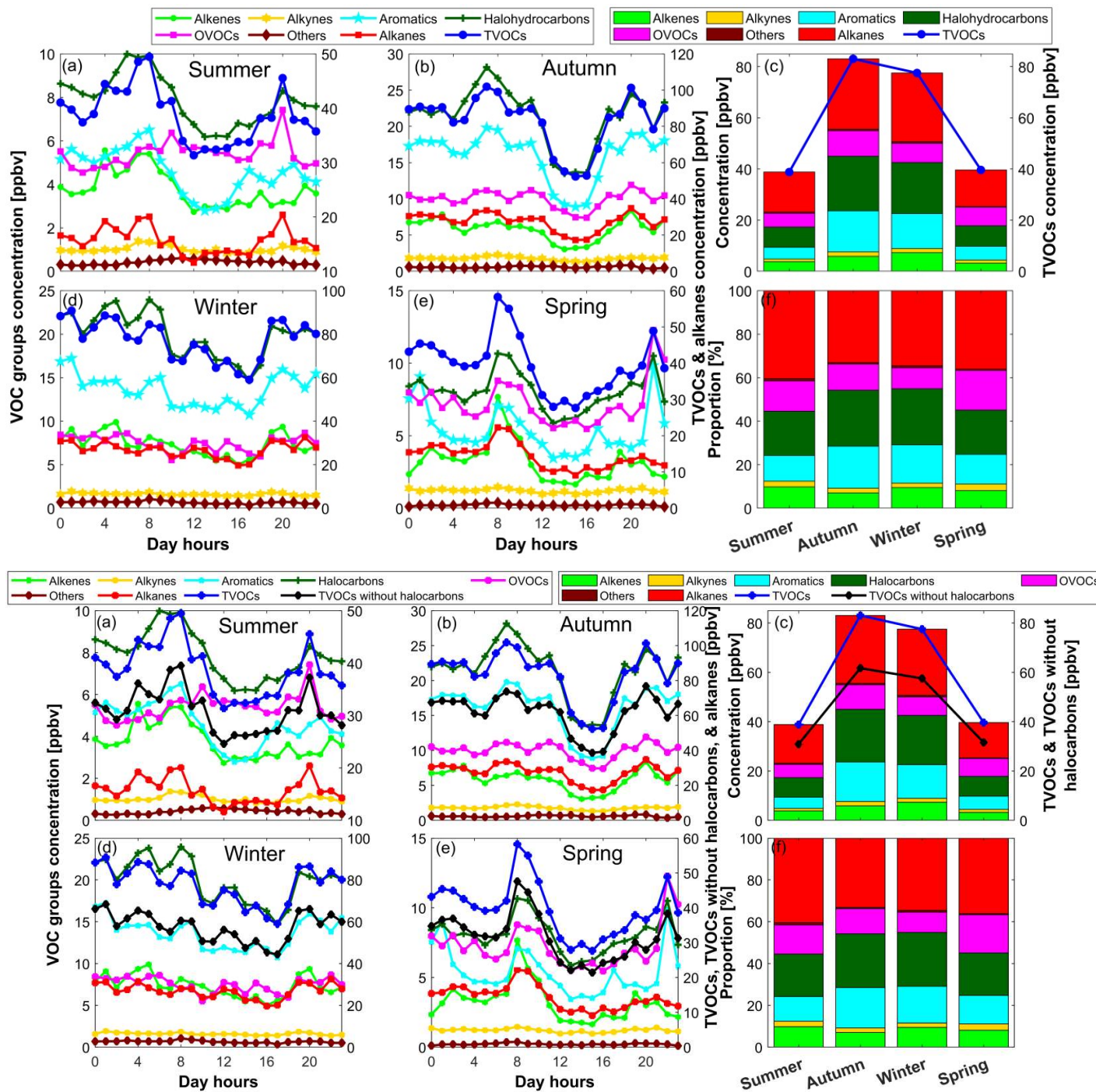


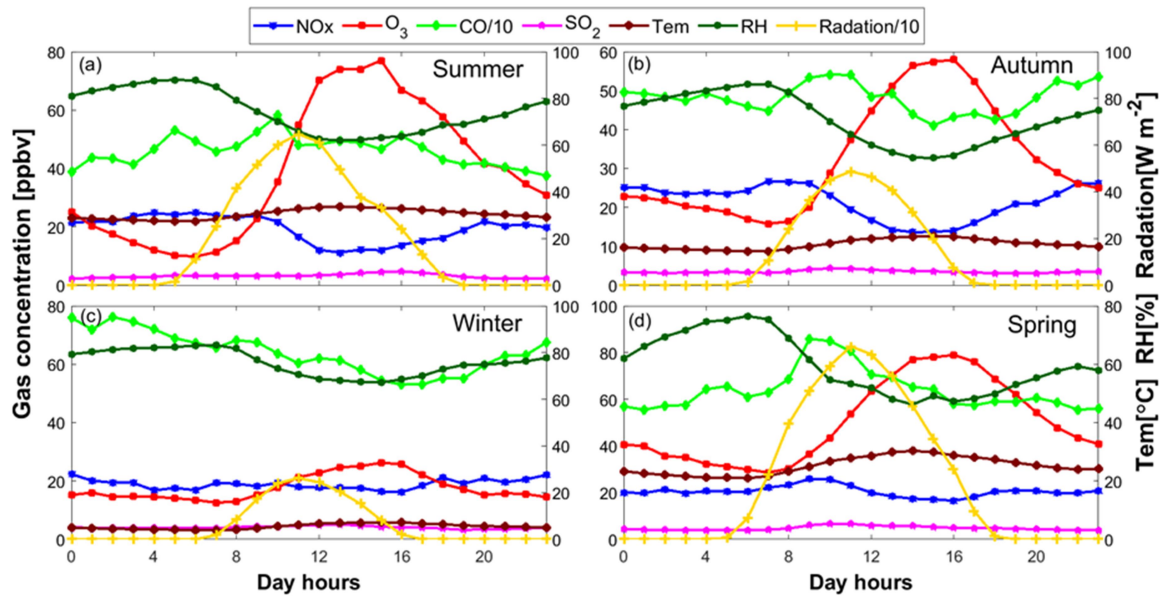
Figure 1: Time series of hourly meteorological parameters, inorganic air pollutants, and TVOCs, and TVOCs without halocarbons concentrations during the observation period at Nanjing. The green, yellow, cyan, and light-green shaded areas indicate summer, autumn, winter, and spring seasons, respectively. The discontinuity of the measured data is due to the instruments failure.

875



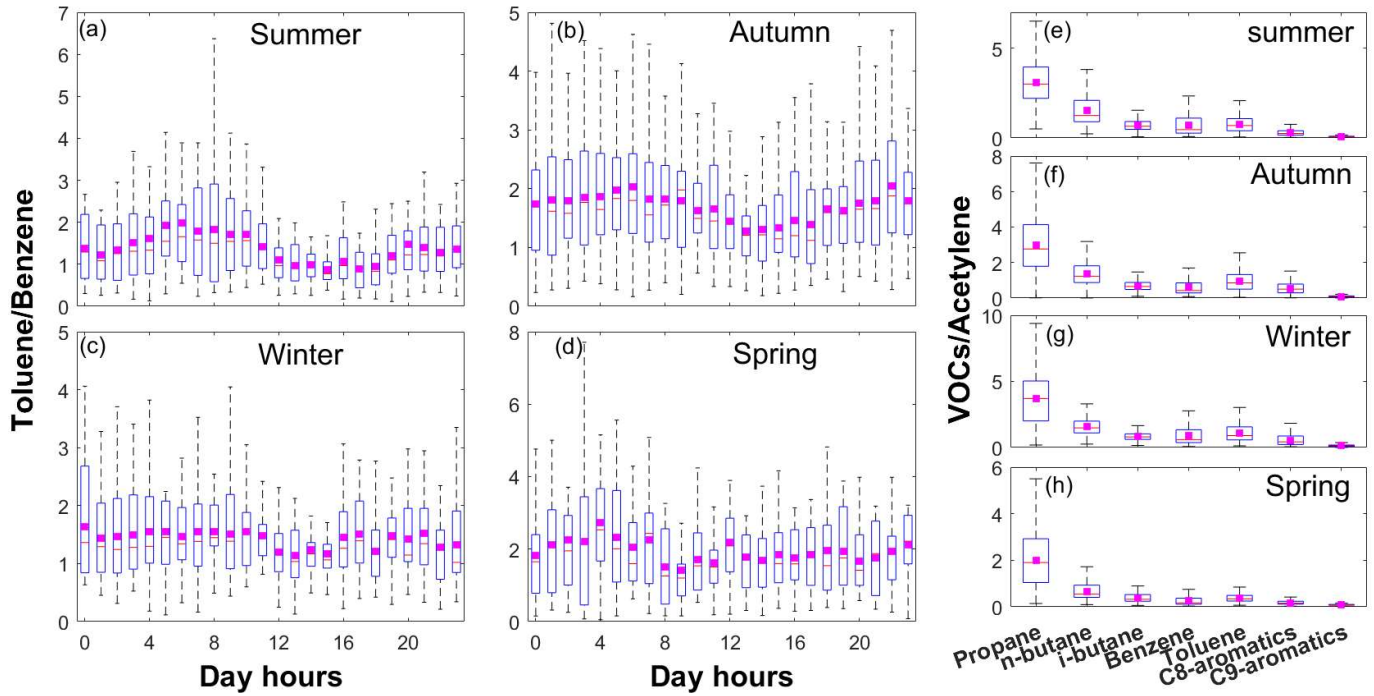
880

Figure 2: Diurnal variations in TVOCs and different VOC-groups, TVOCs, TVOCs without halocarbons concentrations in different seasons (a, b, d, & e) and seasonal variations in average concentrations and proportion of different VOC-groups, TVOCs, TVOCs without halocarbons TVOCs and different VOC-groups (c & f).



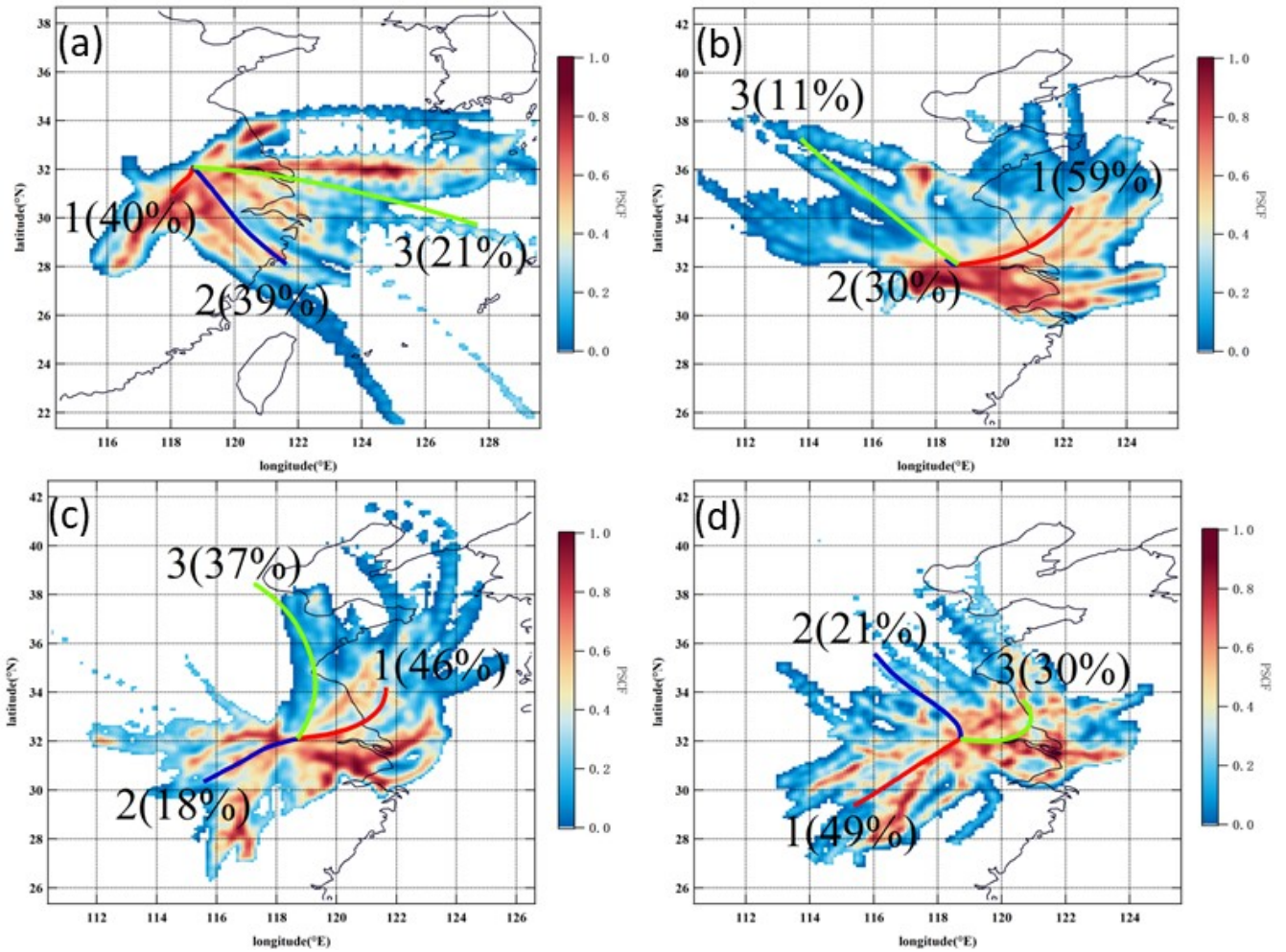
885

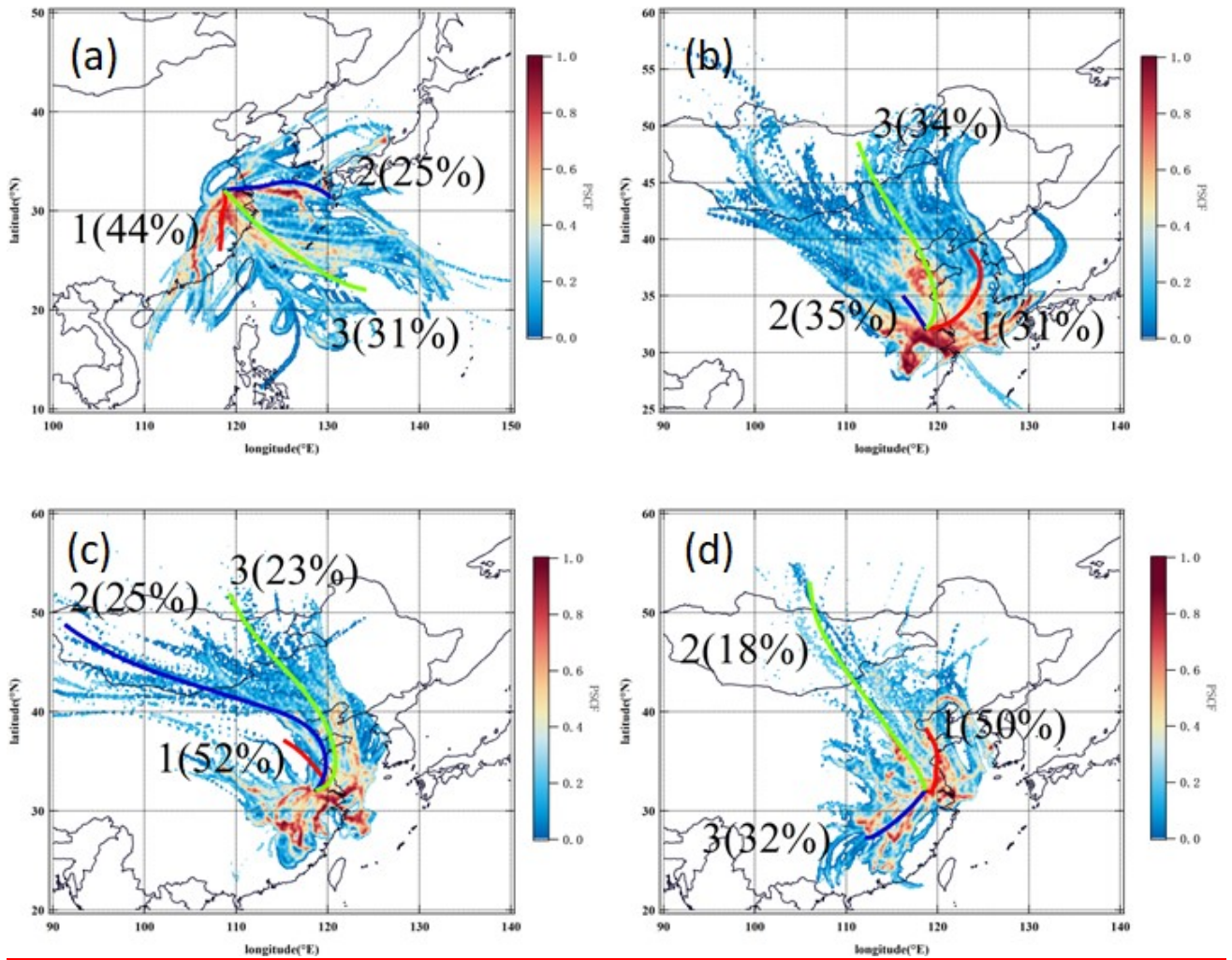
Figure 3: Diurnal variations in weather conditions and NO_x, O₃, CO, and SO₂ concentrations in different seasons. Note that the plotted CO concentrations and solar radiation values are reduced by 10-folds for a better visualization.



890

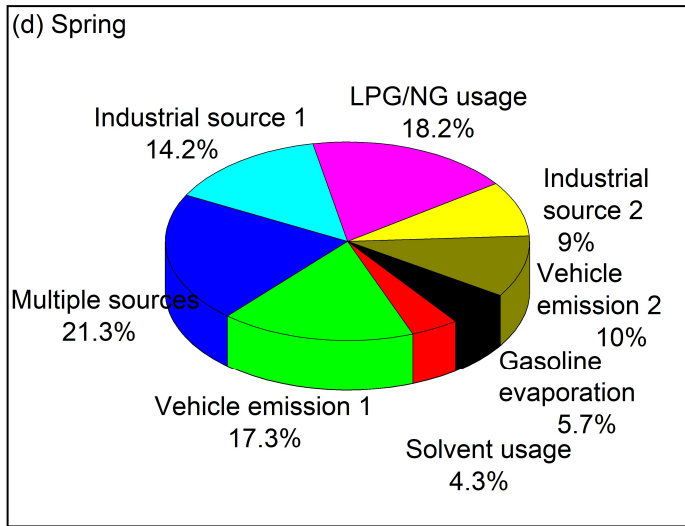
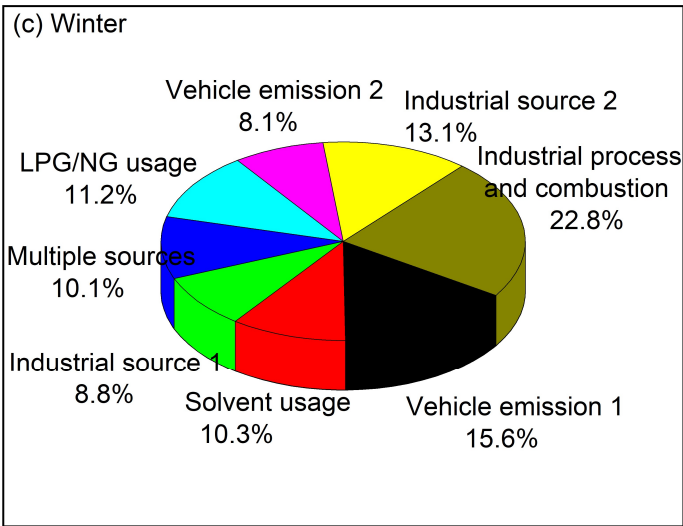
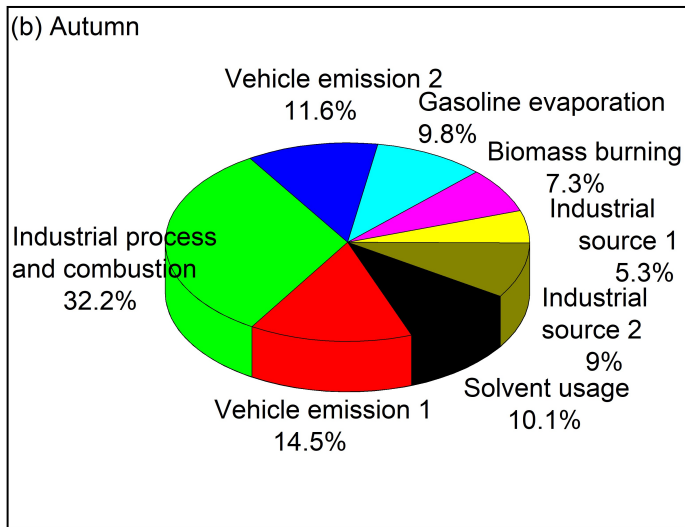
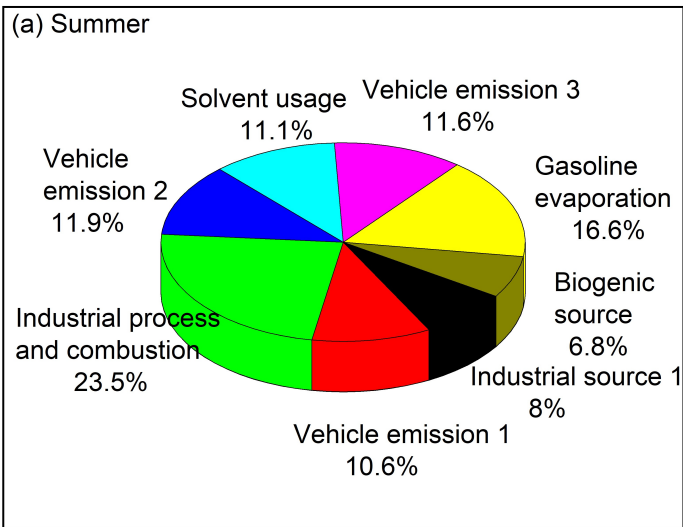
Figure 4: Diurnal variations in toluene/benzene ratios (a, b, c, & d) and in the ratios of different VOCs to acetylene in different seasons (e, f, g, & h). The pink-colored squares in the box-plots represent the average values.

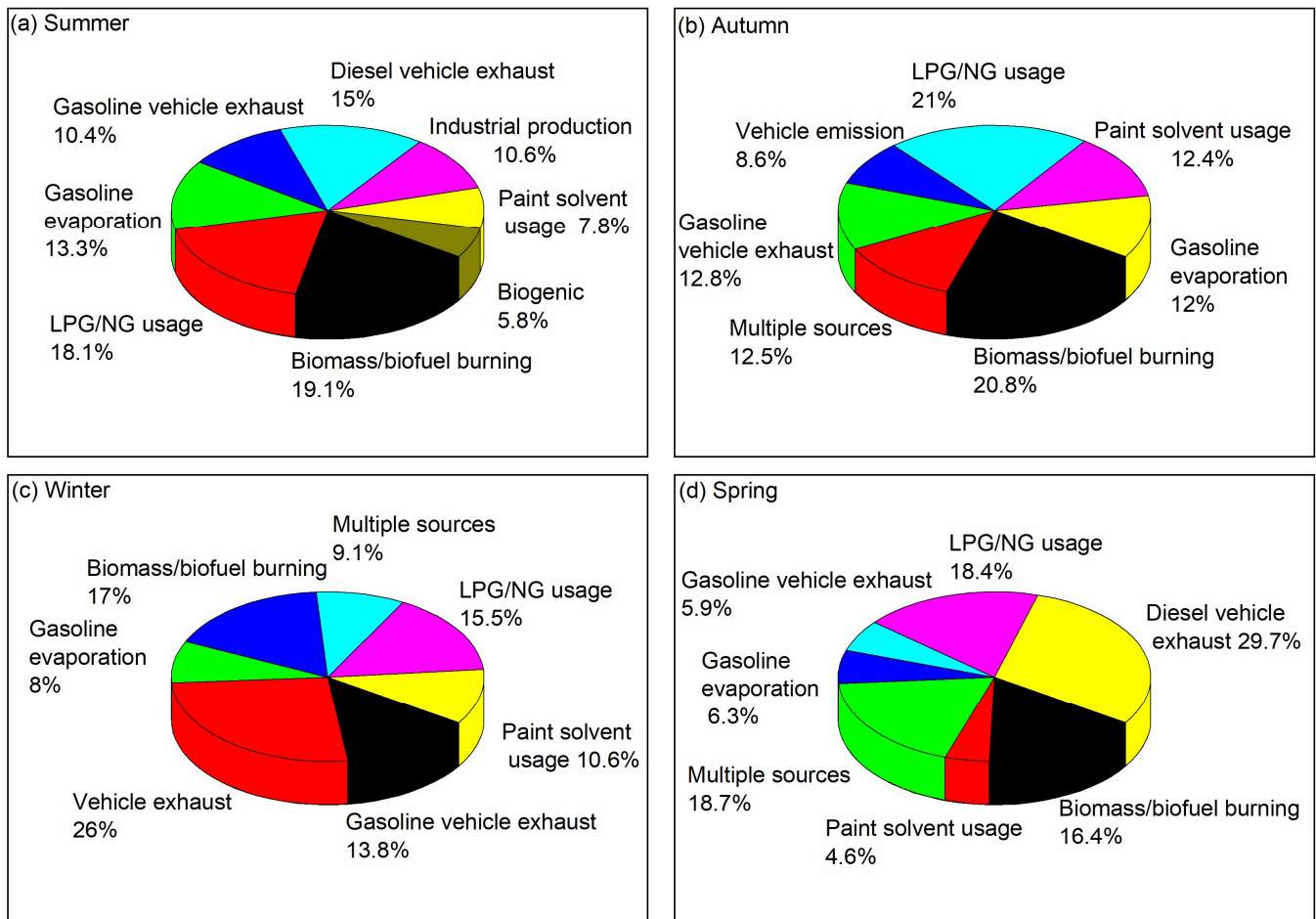




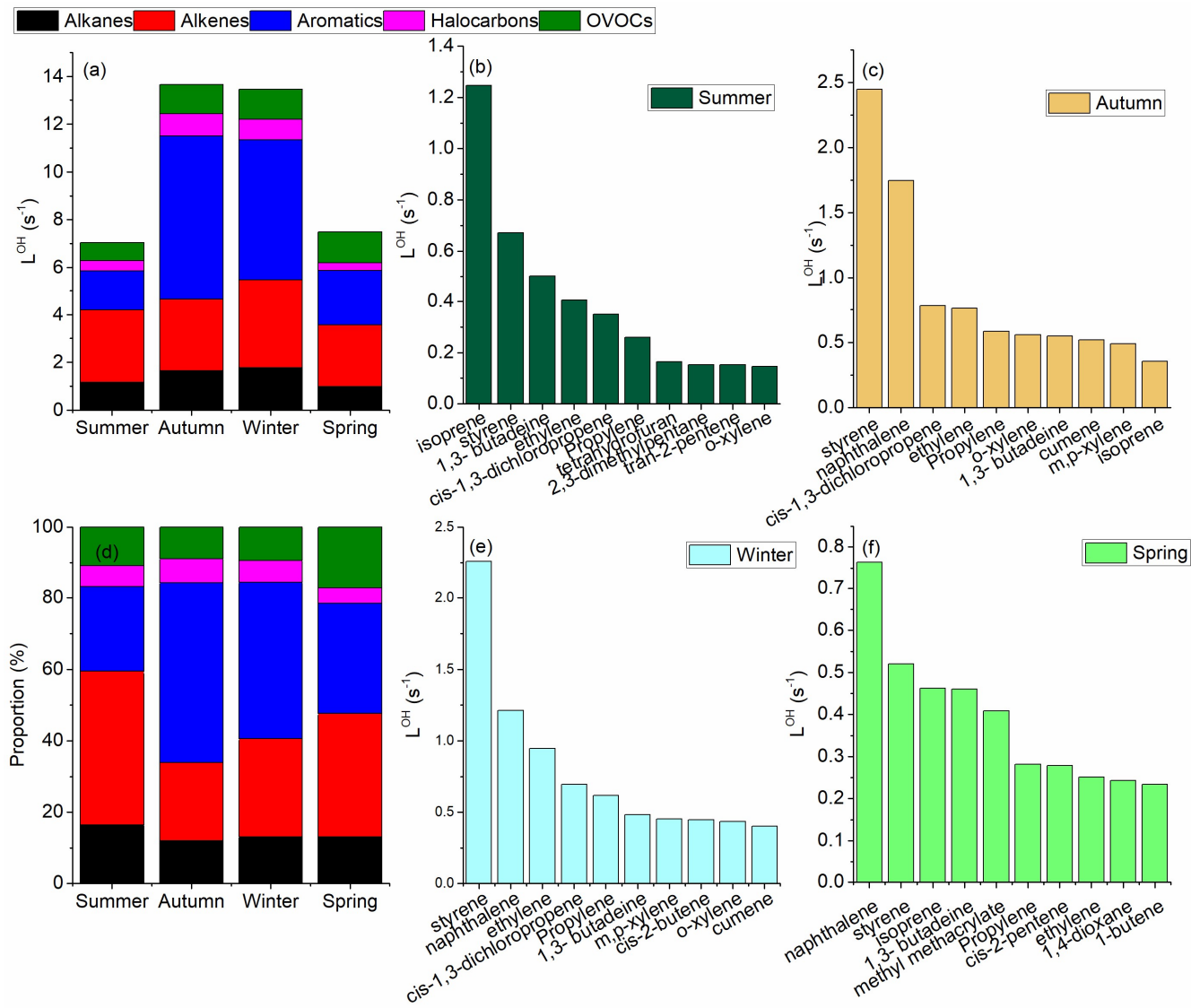
895

Figure 5: Wind cluster and PSCF analysis during (a) summer (b) autumn, (c) winter, and (d) spring based on the 24-72 hours backward air mass trajectories from the study area.





900 **Figure 6: relative contributions of different sources to ambient VOCs in Nanjing industrial area during different seasons**



905

Figure 7: Contribution to OH loss rates of different VOC-groups and the top 10 VOC species in different seasons

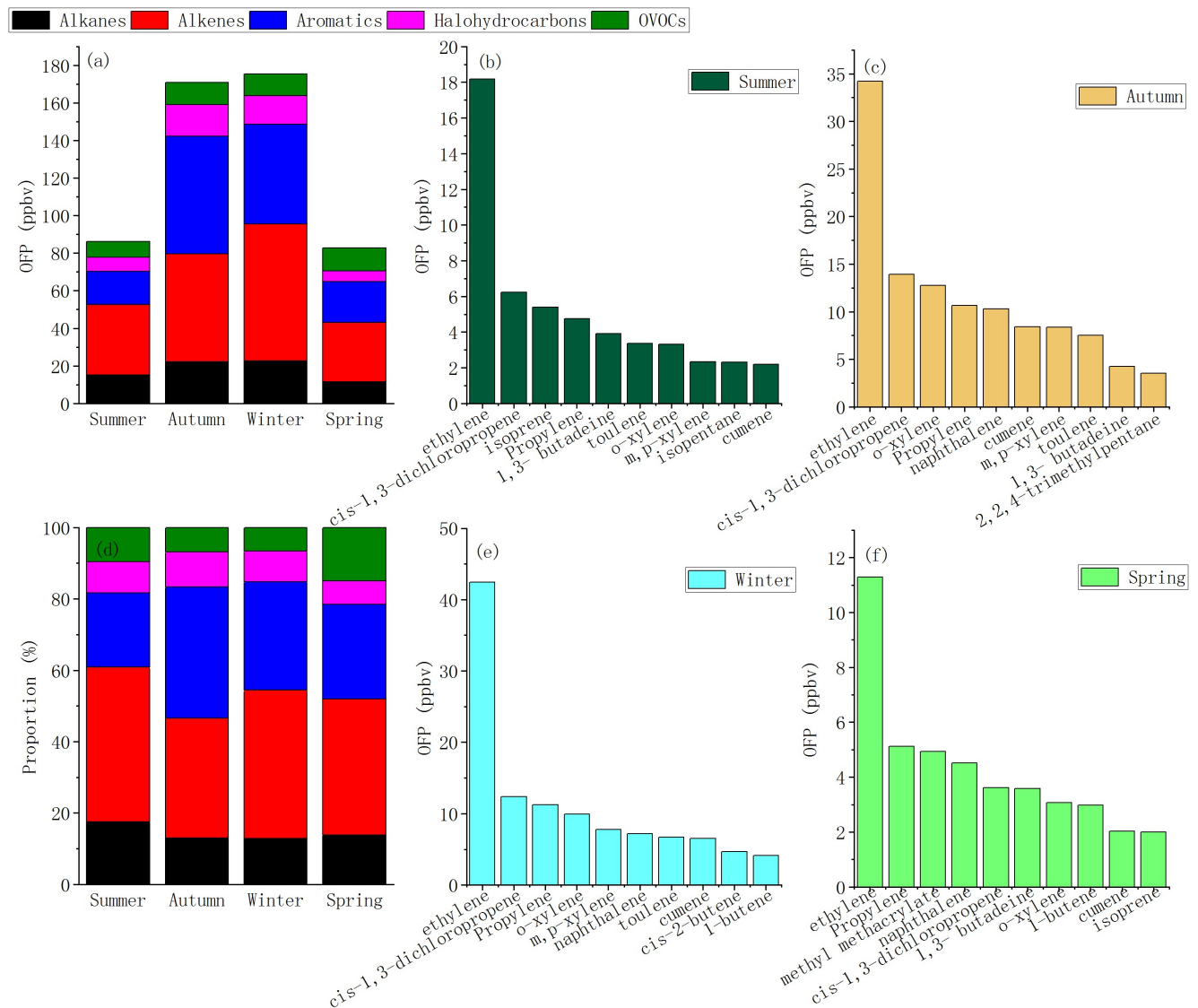


Figure 8: Contribution to ozone formation potential of different VOC groups and the top 10 VOC species in different seasons

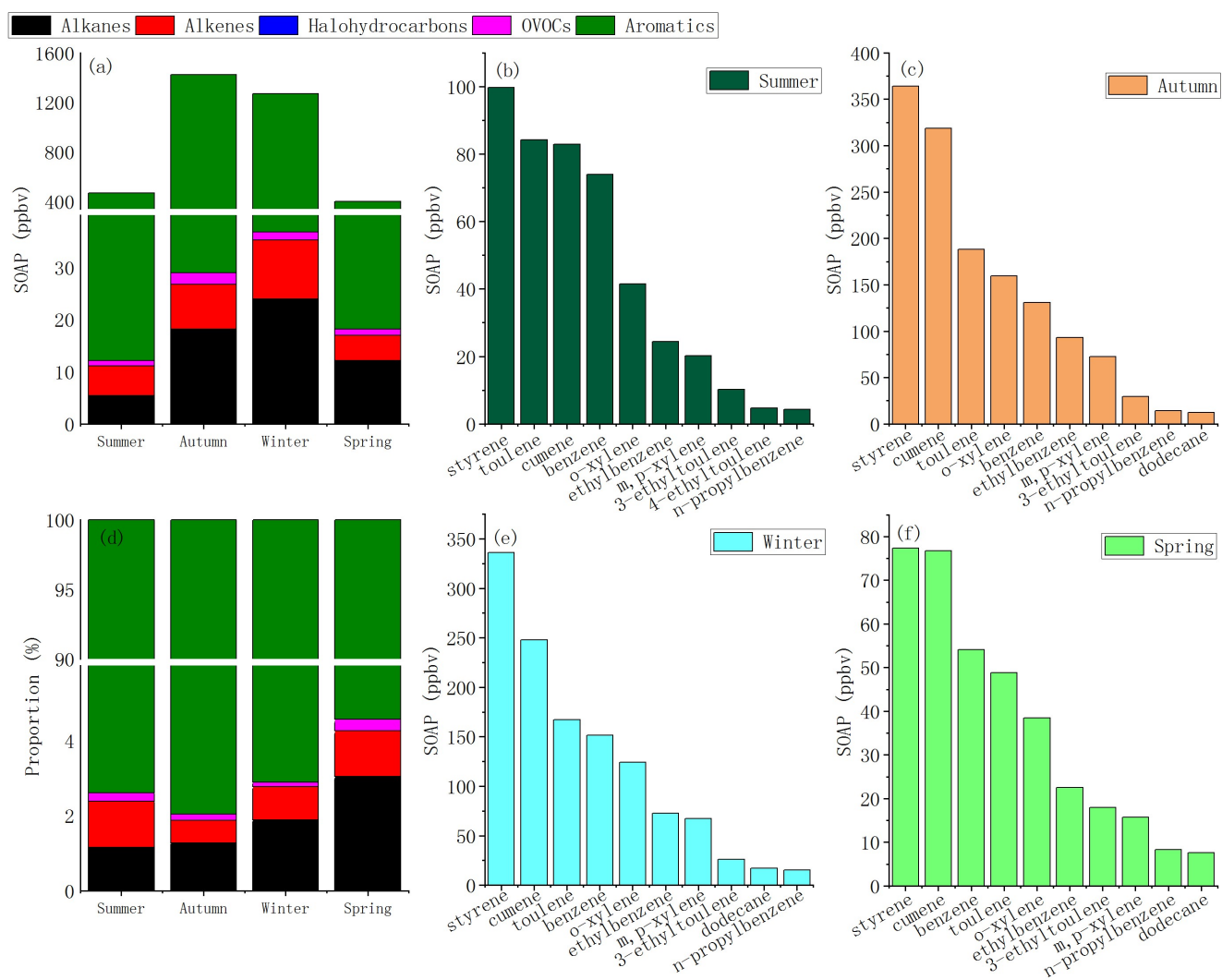


Figure 9: Contribution to secondary organic aerosol formation potential of different VOC groups and the top 10 VOC species in different seasons

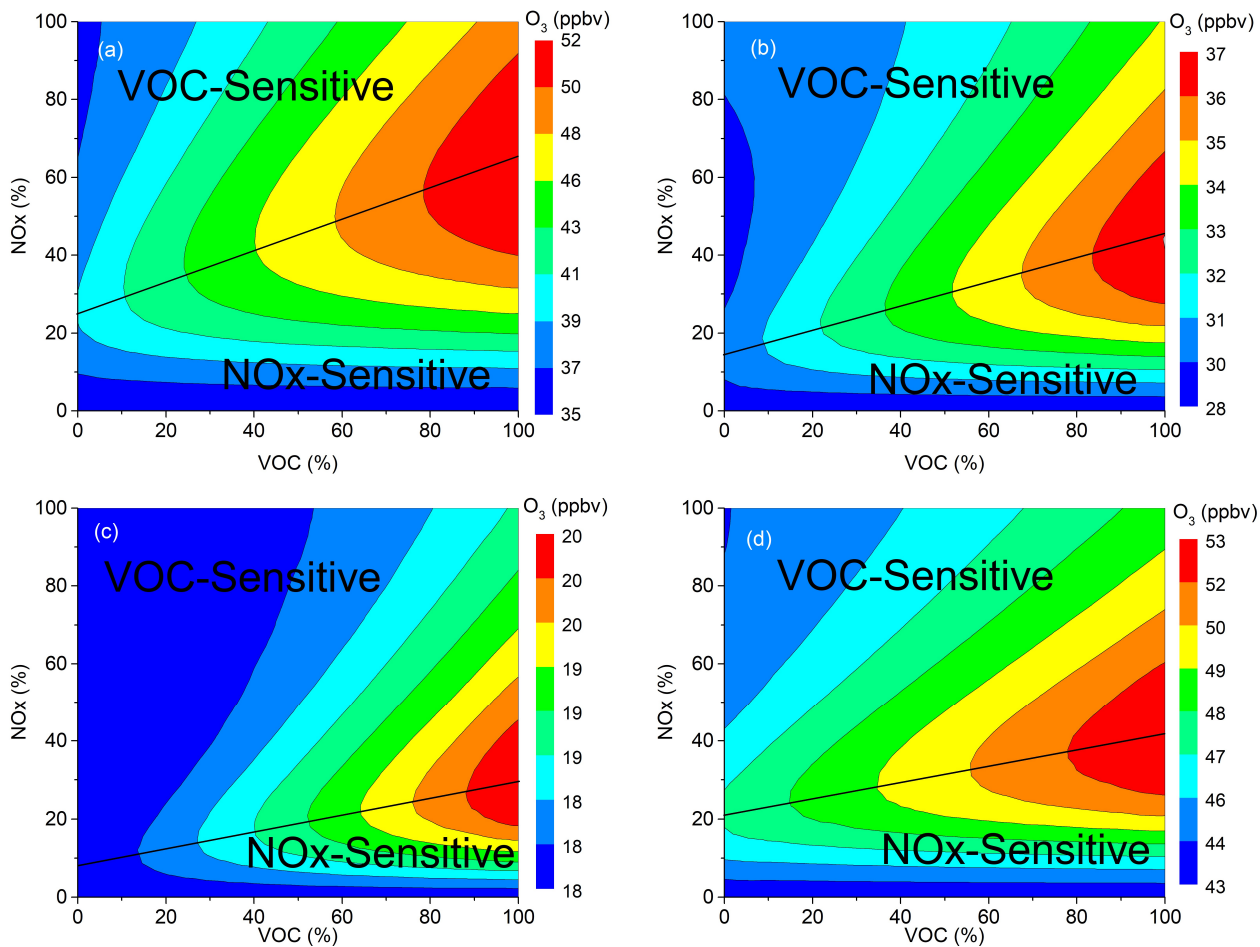


Figure 10: O_3 isopleth diagram for (a) summer (b) autumn, (c) winter, and (d) spring based on percentage changes in VOCs and NO_x concentrations in Nanjing and corresponding modelled O_3 production.

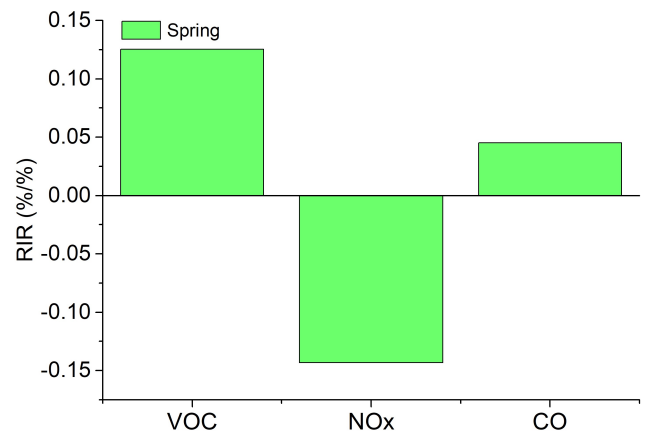
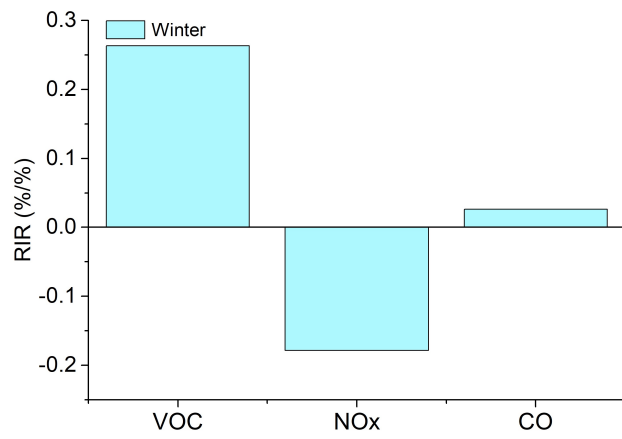
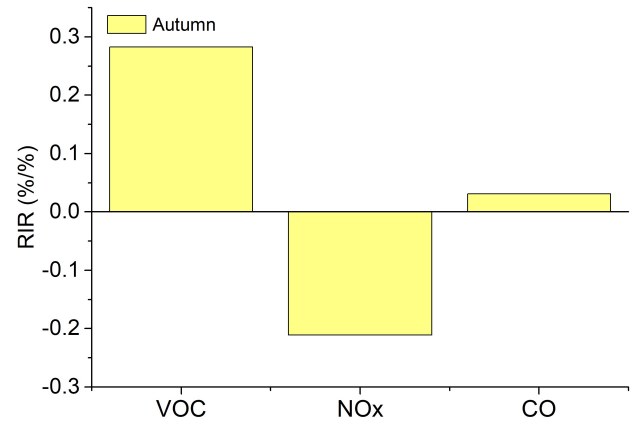
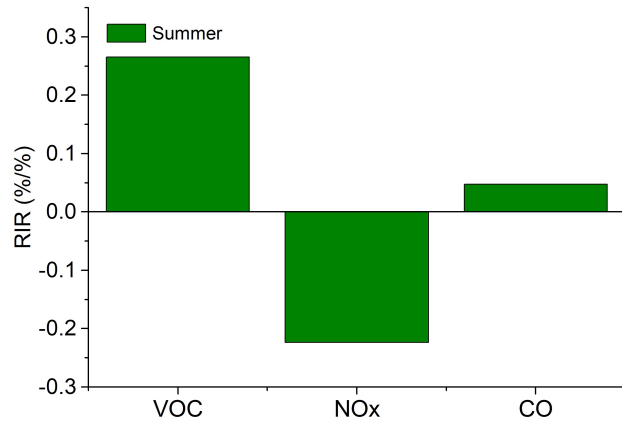


Figure 11: The RIR values of the VOC, NOx, and CO for the different seasons in Nanjing

925

930

935

Supplement

Measurement report: High Contributions of Halohydrocarbon and Aromatic Compounds to Emissions and Chemistry of Atmospheric VOCs in Industrial Area

940 Ahsan Mozaffar^{1,2,3}, Yan-Lin Zhang^{1,2,3*}, Yu-Chi Lin^{1,2,3}, Feng Xie^{1,2,3}, Mei-Yi Fan^{1,2,3}, and Fang
Cao^{1,2,3}

¹Yale-NUIST Center on Atmospheric Environment, International Joint Laboratory on Climate and Environment Change, Nanjing University of Information Science and Technology, Nanjing, 210044, China.

945 ²Key Laboratory Meteorological Disaster; Ministry of Education & Collaborative Innovation Center on Forecast and Evaluation of Meteorological Disaster, Nanjing University of Information Science and Technology, Nanjing, 210044, China.

³Jiangsu Provincial Key Laboratory of Agricultural Meteorology, College of Applied Meteorology, Nanjing University of Information Science & Technology, Nanjing 210044, China.

950 *Correspondence to:* Yan-Lin Zhang (dryanlinzhang@outlook.com)

Table S1: OH reaction rate constant (K^{OH}) of VOCs

Compounds	K^{OH} (Carter, 2010)
ethane	2.54E-13
propane	1.11E-12
isobutane	2.14E-12
n-butane	2.38E-12
isopentane	3.60E-12
n-pentane	3.84E-12
2,2 dimethylbutane	2.27E-12
2,3 dimethyl butane	5.79E-12
2-methyl pentane	5.20E-12
cyclopentane	5.02E-12
3-methylpentane	5.20E-12
n-hexane	5.25E-12
2,4-dimethylpentane	4.77E-12
methylcyclopentane	5.68E-12
isoheptane	6.81E-12
cyclohexane	7.02E-12

2,3-dimethylpentane	7.15E-12
3-methylhexane	7.17E-12
2,2,4-trimethylpentane	3.38E-12
heptane	6.81E-12
methylcyclohexane	9.64E-12
2-methylheptane	8.31E-12
n-octane	8.16E-12
n-nonane	9.75E-12
decane	1.10E-11
n-hendecane	1.23E-11
dodecane	1.32E-11
ethylene	8.15E-12
Propylene	2.60E-11
trans-2-butene	6.32E-11
cis-2-butene	5.58E-11
1-butene	3.11E-11
1,3- butadiene	6.59E-11
1-pentene	3.14E-11
trans-2-pentene	6.70E-11
isoprene	9.96E-11
cis-2-pentene	6.50E-11
1-hexene	3.70E-11
acetylene	7.56E-13
benzene	1.22E-12
toulene	5.58E-12
ethylbenzene	7.00E-12
m,p-xylene	2.31E-11
o-xylene	1.36E-11
styrene	5.80E-11
cumene	6.30E-12
n-propylbenzene	5.80E-12
3-ethyltoulene	1.86E-11
4-ethyltoulene	1.18E-11
mesitylene	5.67E-11
2-ethyltoulene	1.19E-11
1,2,4-trimethylbenzene	3.25E-11
1,2,3-trimethylbenzene	3.27E-11
1,3-diethylbenzene	2.55E-11
1,4-diethylbenzene	1.64E-11
naphthalene	2.30E-11
chloromethane	4.48E-14

vinyl chloride	6.90E-12
methyl bromide	4.12E-14
chloroethene	0
trichlorofloromethane	0
Vinylidene chloride	0
1,1,2-Trichlor-1,2,2-trifluorethan	0
dichloromethane	1.45E-13
trans-1,2-dichloroethylene	0
1,1-dichloroethane	2.60E-13
cis-1,2-dichloroethylene	0
chloroform	1.06E-13
carbon tetrachloride	0
1,2-dichloroethane	2.53E-13
trichloroethylene	2.34E-12
1,2-dichloropropane	4.50E-13
bromodichloromethane	0
trans-1,3-dichloropropene	1.44E-11
cis-1,3-dichloropropene	8.45E-12
1,1,2-trichloroethane	2.00E-13
tetrachloroethylene	0
1,2-dibromoethane	2.27E-13
chlorobenzene	7.70E-13
bromoform	0
1,1,2,2-tetrachloroethane	0
1,3-dichlorobenzene	5.55E-13
1,4 dichlorobebezne	5.55E-13
benzyl chloride	0
1,2-dichlorobenzene	5.55E-13
1,2,4-trichlorobenzene	0
hexachloro-1,3-butadiene	0
carbon disulfide	2.76E-12
Acrolein	1.99E-11
acetone	1.91E-13
isopropanol	5.09E-12
MTBE	0
vinyl acetate	3.16E-11
MEK	1.20E-12
ethyl acetate	1.60E-12
tetrahydrofuran	1.61E-11
methyl methacrylate	5.25E-11
1,4-dioxane	3.83E-11

4-methyl-2-pentanone	1.27E-11
2-hexanone	9.10E-12

954 **Table S2: VOC concentrations measured in the industrial area in Nanjing. VOC concentrations observed in previous studies**
 955 **in Nanjing are also listed.**

Compounds	Current study										(An et al., 2017), Nanjing		(Wu et al., 2020), Nanjing
	Summer		Autumn		Winter		Spring		Yearly		Summer	Winter	Yearly
	Mean	Std	Mean	Std	Mean	Std	Mean	Std	Mean	Std	Mean	Mean	Mean
ethane	2.81	0.58	8.06	1.77	7.66	1.39	4.76	1.25	5.82	2.49	2.76	7.66	2.89
propane	3.12	0.63	6.09	1.21	4.92	0.91	2.73	0.92	4.22	1.57	1.70	4.51	3.29
isobutane	0.75	0.16	1.25	0.26	1.16	0.15	0.48	0.14	0.91	0.36	1.04	2.25	0.9
n-butane	1.75	0.39	2.61	0.63	2.32	0.26	0.87	0.29	1.89	0.76	1.09	2.35	1.53
isopentane	1.59	0.29	1.56	0.47	1.63	0.31	0.42	0.19	1.30	0.59	0.86	1.13	1.26
n-pentane	0.66	0.17	1.06	0.29	1.36	0.25	0.31	0.10	0.85	0.46	0.50	0.86	0.78
2,2 dimethylbutane	0.08	0.01	0.06	0.01	0.06	0.01	0.06	0.01	0.06	0.01	0.28	0.03	0.04
2,3 dimethyl butane	0.13	0.03	0.18	0.03	0.11	0.00	0.20	0.02	0.16	0.04	0.12	0.35	0.04
2-methyl pentane	0.26	0.08	0.32	0.10	0.44	0.11	0.29	0.06	0.33	0.08	0.25	0.41	0.16
cyclopentane	0.15	0.03	0.10	0.02	0.08	0.01	0.22	0.03	0.14	0.06	0.08	0.12	0.08
3-methylpentane	0.25	0.06	0.38	0.09	0.37	0.12	0.25	0.08	0.31	0.07	0.22	0.31	0.26
n-hexane	0.17	0.04	0.33	0.09	0.41	0.17	0.21	0.06	0.28	0.11	0.41	0.48	0.47
2,4- dimethylpentane	0.06	0.00	0.06	0.01	0.06	0.00	0.13	0.01	0.08	0.03	0.05	0.08	0.01

methylcyclopentane	0.12	0.03	0.16	0.04	0.14	0.04	0.13	0.03	0.14	0.02	0.08	0.13	0.26
isoheptane	0.13	0.04	0.12	0.04	0.11	0.04	0.16	0.03	0.13	0.02			
cyclohexane	0.44	0.29	0.37	0.15	0.43	0.31	0.21	0.13	0.36	0.10	0.41	0.60	0.15
2,3-dimethylpentane	0.86	0.59	0.73	0.30	0.85	0.63	0.42	0.25	0.72	0.21	0.11	0.20	0.02
3-methylhexane	0.10	0.02	0.12	0.03	0.09	0.02	0.14	0.02	0.11	0.02	0.04	0.05	0.08
2,2,4-trimethylpentane	1.59	0.37	2.81	0.82	3.26	0.78	1.16	0.74	2.21	0.99	0.03	0.02	0.03
heptane	0.10	0.01	0.12	0.02	0.12	0.01	0.10	0.01	0.11	0.01	1.92	0.2	0.11
methylcyclohexane	0.18	0.02	0.18	0.04	0.19	0.03	0.16	0.03	0.18	0.01	0.08	0.12	0.08
2-methylheptane	0.08	0.00	0.08	0.01	0.08	0.00	0.17	0.01	0.10	0.04	0.01	0.05	0.02
n-octane	0.09	0.01	0.08	0.01	0.09	0.01	0.20	0.01	0.11	0.06	0.19	0.21	0.05
n-noane	0.06	0.00	0.08	0.02	0.08	0.02	0.07	0.00	0.07	0.01	0.03	0.05	0.03
decane	0.05	0.00	0.06	0.01	0.06	0.01	0.05	0.00	0.06	0.01	0.05	0.06	0.04
n-hendecane	0.04	0.01	0.16	0.01	0.22	0.01	0.17	0.01	0.15	0.07	0.06	0.09	0.02
dodecane	0.08	0.00	0.36	0.02	0.50	0.01	0.22	0.02	0.29	0.18	0.07	0.13	0.03
ethylene	2.02	0.58	3.80	0.89	4.71	1.09	1.25	0.71	2.95	1.59	3.08	6.62	1.21
Propylene	0.41	0.34	0.91	0.46	0.97	0.31	0.44	0.58	0.68	0.30	0.98	2.09	0.70
trans-2-butene	0.02	0.00	0.06	0.02	0.23	0.01	0.03	0.01	0.09	0.10	0.07	0.14	0.07
cis-2-butene	0.07	0.00	0.16	0.03	0.33	0.03	0.09	0.01	0.16	0.12	0.06	0.10	0.05
1-butene	0.07	0.00	0.10	0.02	0.43	0.02	0.31	0.13	0.22	0.17	0.18	0.23	0.15

1,3- butadiene	0.31	0.07	0.34	0.05	0.30	0.03	0.28	0.00	0.31	0.02			
1-pentene	0.16	0.03	0.14	0.03	0.08	0.03	0.10	0.03	0.12	0.04	0.04	0.05	0.04
tran-2-pentene	0.09	0.03	0.06	0.02	0.05	0.01	0.09	0.02	0.07	0.02	0.03	0.04	0.03
isoprene	0.51	0.37	0.15	0.06	0.09	0.02	0.19	0.02	0.23	0.19	0.58	0.07	0.18
cis-pentene	0.07	0.02	0.06	0.01	0.07	0.01	0.17	0.02	0.09	0.05	0.03	0.02	0.02
1-hexene	0.05	0.03	0.06	0.02	0.06	0.03	0.24	0.01	0.10	0.09	0.03	0.02	0.01
acetylene	1.02	0.15	1.77	0.24	1.59	0.15	1.20	0.13	1.40	0.35	2.63	6.46	
benzene	0.80	0.19	1.41	0.41	1.63	0.39	0.58	0.37	1.10	0.50	1.86	3.21	0.82
toulene	0.84	0.40	1.88	0.51	1.67	0.31	0.49	0.12	1.22	0.66	1.47	3.20	1.07
ethylbenzene	0.22	0.05	0.83	0.21	0.65	0.15	0.20	0.10	0.48	0.32	1.27	1.79	0.43
m,p-xylene	0.24	0.07	0.86	0.24	0.80	0.17	0.19	0.07	0.52	0.36	0.46	0.59	0.67
o-xylene	0.43	0.09	1.67	0.42	1.30	0.29	0.40	0.21	0.95	0.63	0.28	0.39	0.21
styrene	0.47	0.15	1.71	0.49	1.58	0.35	0.36	0.15	1.03	0.71	0.17	0.30	0.12
cumene	0.87	0.19	3.34	0.84	2.60	0.59	0.80	0.41	1.90	1.27			
n-propylbenzene	0.04	0.01	0.13	0.02	0.14	0.01	0.08	0.11	0.10	0.05	0.09	0.08	0.03
3-ethyltoulene	0.10	0.02	0.29	0.06	0.26	0.05	0.18	0.21	0.21	0.09	0.05	0.05	0.03
4-ethyltoulene	0.07	0.00	0.08	0.01	0.08	0.01	0.10	0.06	0.08	0.01	0.19	0.29	0.03
mesitylene	0.03	0.00	0.06	0.02	0.08	0.03	0.04	0.00	0.05	0.02			
2-ethyltoulene	0.04	0.01	0.07	0.02	0.07	0.02	0.06	0.07	0.06	0.02	0.51	0.08	
1,2,4-trimethylbenzen e	0.06	0.01	0.06	0.02	0.08	0.03	0.13	0.11	0.08	0.03	0.33	0.42	0.09

1,2,3-trimethylbenzene	0.08	0.01	0.20	0.03	0.22	0.01	0.10	0.01	0.15	0.07	0.05	0.05	0.05
1,3-diethylbenzene	0.09	0.00	0.18	0.02	0.17	0.01	0.16	0.01	0.15	0.04	0.03	0.05	0.01
1,4-diethylbenzene	0.09	0.00	0.17	0.02	0.20	0.01	0.17	0.01	0.16	0.05	0.04	0.10	0.04
naphthalene	0.13	0.02	3.09	0.98	2.14	0.22	1.35	0.29	1.68	1.25			
chloromethane	0.16	0.02	0.56	0.08	1.21	0.33	0.15	0.01	0.52	0.50			
vinyl chloride	0.05	0.00	0.07	0.02	0.09	0.02	0.16	0.01	0.09	0.05			
methyl bromide	0.04	0.00	0.05	0.01	0.04	0.01	0.03	0.00	0.04	0.01			
chloroethene	0.08	0.01	0.08	0.02	0.10	0.03	0.05	0.01	0.08	0.02			
trichlorofluoromethane	0.23	0.01	0.18	0.01	0.30	0.02	0.21	0.04	0.23	0.05			
Vinylidene chloride	0.05	0.01	0.05	0.01	0.04	0.00	0.05	0.01	0.05	0.00			
1,1,2-Trichloro-1,2,2-trifluoroethane	0.08	0.00	0.08	0.01	0.10	0.00	0.08	0.01	0.08	0.01			
dichloromethane	1.26	0.09	3.09	0.54	2.62	0.47	1.97	0.53	2.23	0.80			
trans-1,2-dichloroethylene	0.05	0.00	0.05	0.01	0.05	0.01	0.14	0.01	0.07	0.05			
1,1-dichloroethane	0.33	0.08	0.65	0.18	0.82	0.34	0.41	0.13	0.55	0.22			
cis-1,2-dichloroethylene	0.07	0.00	0.07	0.01	0.03	0.00	0.20	0.01	0.09	0.07			

chloroform	0.17	0.02	0.57	0.16	0.53	0.18	0.18	0.04	0.36	0.22
carbon tetrachloride	0.12	0.01	0.18	0.02	0.17	0.03	0.18	0.02	0.16	0.03
1,2- dichloroethane	0.95	0.14	3.19	0.40	2.95	0.43	1.15	0.31	2.06	1.17
trichloroethylene	0.13	0.02	0.14	0.02	0.10	0.02	0.06	0.00	0.11	0.04
1,2- dichloropropane	0.57	0.21	1.48	0.53	0.96	0.23	0.14	0.05	0.79	0.57
bromodichlorom ethane	0.06	0.00	0.03	0.01	0.03	0.00	0.06	0.00	0.04	0.01
trans-1,3- dichloropropene	0.10	0.00	0.08	0.01	0.13	0.00	0.17	0.01	0.12	0.04
cis-1,3- dichloropropene	1.68	0.79	3.76	1.02	3.35	0.62	0.98	0.23	2.44	1.33
1,1,2- trichloroethane	0.06	0.01	0.12	0.04	0.11	0.07	0.05	0.05	0.09	0.03
tetrachloroethyle ne	0.06	0.00	0.09	0.02	0.08	0.02	0.06	0.01	0.07	0.01
1,2- dibromoethane	0.03	0.00	0.02	0.01	0.02	0.00	0.02	0.00	0.02	0.01
chlorobenzene	0.31	0.18	1.89	0.91	1.73	1.14	0.20	0.16	1.03	0.90
bromoform	0.02	0.00	0.02	0.01	0.02	0.00	0.02	0.00	0.02	0.00
1,1,2,2- tetrachloroethan e	0.94	0.30	3.43	0.97	3.16	0.70	0.73	0.30	2.06	1.43
1,3-	0.02	0.00	0.09	0.03	0.14	0.05	0.04	0.01	0.07	0.05

dichlorobenzene										
1,4 dichlorobezne	0.11	0.01	0.65	0.20	0.40	0.05	0.09	0.01	0.31	0.27
benzyl chloride	0.12	0.02	0.10	0.05	0.13	0.07	0.24	0.23	0.15	0.06
1,2- dichlorobenzene	0.03	0.01	0.25	0.11	0.15	0.04	0.08	0.01	0.13	0.10
1,2,4- trichlorobenzene	0.04	0.00	0.17	0.04	0.25	0.01	0.14	0.02	0.15	0.09
hexachloro-1,3- butadiene	0.02	0.00	0.17	0.04	0.15	0.04	0.02	0.00	0.09	0.08
carbon disulfide	0.42	0.11	0.59	0.13	0.66	0.15	0.21	0.07	0.47	0.20
Acrolein	0.09	0.02	0.07	0.02	0.05	0.01	0.07	0.02	0.07	0.01
acetone	1.60	0.29	2.98	0.25	1.94	0.22	2.61	0.61	2.28	0.63
isopropanol	0.46	0.07	2.34	0.60	1.28	0.34	0.44	0.10	1.13	0.90
MTBE	0.37	0.11	0.66	0.23	0.35	0.11	0.35	0.13	0.43	0.15
vinyl acetate	0.17	0.04	0.33	0.09	0.42	0.18	0.26	0.08	0.30	0.11
MEK	0.69	0.06	1.14	0.10	0.73	0.09	0.77	0.43	0.84	0.21
ethyl acetate	1.06	0.17	1.56	0.25	1.43	0.18	1.34	0.95	1.35	0.21
tetrahydrofuran	0.41	0.56	0.08	0.11	0.43	0.45	0.24	0.03	0.29	0.16
methyl methacrylate	0.11	0.01	0.21	0.01	0.20	0.01	0.32	0.00	0.21	0.09
1,4-dioxane	0.05	0.00	0.07	0.01	0.09	0.00	0.26	0.01	0.12	0.10
4-methyl-2- pentanone	0.23	0.08	0.31	0.07	0.28	0.06	0.30	0.03	0.28	0.03

2-hexanone	0.15	0.00	0.23	0.01	0.28	0.01	0.29	0.02	0.23	0.07
TVOC	38.81	10.21	83.05	20.07	77.51	16.77	39.62	13.12	59.75	28.57

S1. Source apportionment of VOCs

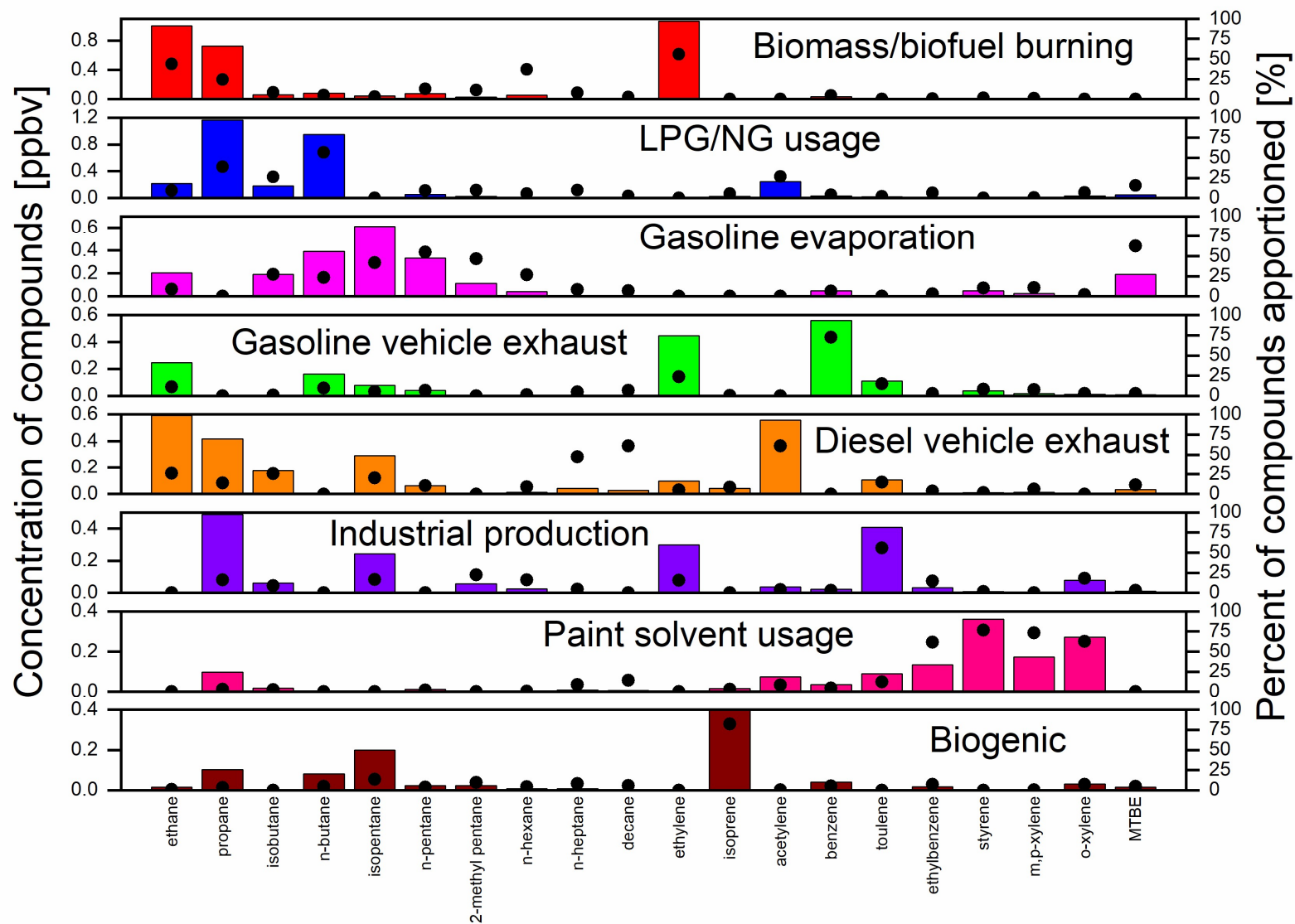
Figure S1 shows the source profile of summertime VOCs obtained from the PMF model. The resolved factors were identified as biomass/biofuel burning, LPG/NG usage, gasoline evaporation, gasoline vehicle exhaust, diesel vehicle exhaust, industrial production, paint solvent usage, and biogenic source. Factor 1 was characterized by high concentrations of ethane and ethylene. These compounds are tracers of incomplete combustion which emitted from vehicle exhaust and biomass/biofuel burning (An et al., 2017). Benzene, toluene, pentane, and decane concentrations were low in factor 1, therefore, it was identified as biomass/biofuel burning. Factor 2 was distinguished by a significant presence of LPG/NG VOCs propane, isobutene, and n-butane (Shao et al., 2016). So, factor 2 was identified as LPG/NG usage. Factor 3 was dominated by high concentrations of isopentane, n-pentane, and MTBE. Therefore, factor 3 was identified as gasoline evaporation (Song et al., 2018; Wang et al., 2016). Factor 4 possessed high concentrations of vehicle exhaust VOCs benzene and toluene (Song et al., 2018). Although these VOCs are also emitted by industrial processes, the contribution of benzene was several folds higher than toluene in this factor. Therefore, factor 4 was related to vehicle exhaust emission and it was assigned to gasoline vehicle exhaust (An et al., 2017). Factor 5 was characterized by high concentrations of acetylene, n-heptane, and decane. These are related to vehicle emission, especially diesel vehicle exhaust emission as diesel engine produce more acetylene than the gasoline engine does (Song et al., 2018; An et al., 2017). Therefore, factor 5 was attributed to diesel vehicle exhaust. Factor 6 was dominated by toluene and the sampling site was beside an industrial area. So, we identified this factor as industrial production. Due to the high contribution of o-xylene, m,p-xylene, ethylbenzene and styrene, factor 7 was assigned to paint solvent usage sources (Li et al., 2018). Factor 8 was attributed to the biogenic source, which was mainly distinguished by a high concentration of isoprene (Song et al., 2018).

During autumn, the possible VOC sources were biomass/biofuel burning, multiple sources, gasoline vehicle exhaust, vehicle emission, LPG/NG usage, paint solvent usage and gasoline evaporation (Fig.S2). Factor 1 was represented by a high concentration of ethane and ethylene, so, it was identified as biomass/biofuel burning (An et al., 2017). Factor 2 was dominated by isoprene, n-heptane, decane, and acetylene. Among these compounds, isoprene is mainly emitted by trees and the rest of the compounds are related to diesel vehicle exhaust emission. Therefore,

Factor 2 was identified as multiple sources. Factor 3 was identified as gasoline vehicle exhaust due to the high contribution of benzene and a relatively small contribution of toluene. In factor 3, benzene was several folds higher than toluene. The 4th factor was mainly composed of vehicle emission-related compounds 2-methyl pentane, n-hexane, n-heptane, n-pentane, and isopentane, therefore, identified as vehicle emission (Song et al., 2018). Factor 5 was assigned to LPG/NG usage as propane, isobutene, and n-butane were the main contributor to it (Shao et al., 2016). Factor 6 was characterized by a high concentration of o-xylene, m,p-xylene, ethylbenzene and styrene, which are typical tracer of paint solvent usage. Factor 7 was identified as gasoline evaporation, it was dominated by high concentrations of isopentane, n-pentane, and MTBE (Song et al., 2018).

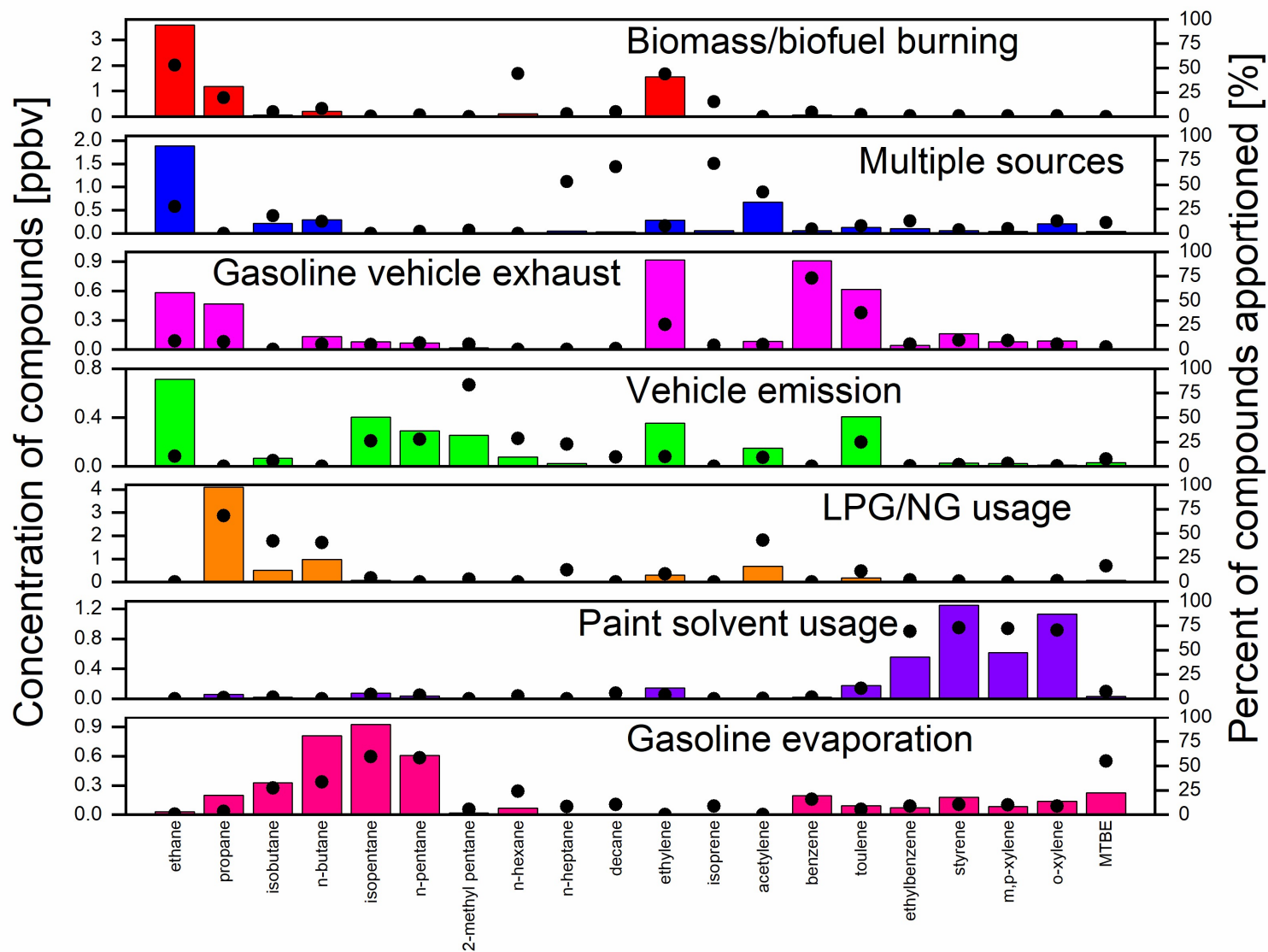
During winter, the source factors were identified as gasoline vehicle exhaust, vehicle exhaust, gasoline evaporation, biomass/biofuel burning, multiple sources, LPG/NG usage, and paint solvent usage (Fig. S3). Factor 1 was assigned to gasoline vehicle exhaust; it was dominated by benzene and toluene and the contribution of benzene was twice of toluene. Factor 2 was represented by a high concentration of isobutene, n-butane, acetylene, ethylene, ethane, n-heptane and decane. Isobutene and n-butane are related to LPG/NG usage, but, the contribution of propane was zero in factor 2. Acetylene, ethylene, and ethane emitted from combustion sources like vehicle exhaust and biomass burning. Decane and n-heptane are related to vehicle emission. By considering the above information, factor 2 was identified as vehicle exhaust. Factor 3 was identified as gasoline evaporation and it was characterized by high concentrations of isopentane and n-pentane. Factor 4 was characterized by a high contribution of ethylene and ethane; therefore, it was identified as biomass/biofuel burning. Factor 5 was characterized by high concentrations of isoprene, propane, n-hexane and n-heptane. Propane is related to LPG/NG usage, isoprene mainly emitted from trees (evergreen trees in winter), and n-hexane and n-heptane are related to vehicle emission. By considering the above information, factor 5 was assigned to multiple sources. Factor 6 was dominated by high concentrations of propane. Therefore, it was identified as LPG/NG usage. Factor 7 was identified as paint solvent usage due to the high contribution of o-xylene, m,p-xylene, ethylbenzene and styrene (Zhang et al., 2018; Song et al., 2020).

1015 During spring, the possible VOC sources were biomass/biofuel burning, paint solvent usage,
multiple sources, gasoline evaporation, gasoline vehicle exhaust, LPG/NG usage, and diesel
vehicle exhaust (Fig. S4). Factor 1 was identified as a biomass/biofuel burning source for the
high loading of ethylene and ethane and relatively lower contribution from the vehicle emission
related compounds. Due to the high contribution of o-xylene, styrene, m,p-xylene, and
1020 ethylbenzene, factor 2 was assigned to paint solvent usage sources (Li et al., 2018). Factor 3 had
a high contribution of isoprene, n-hexane, n-heptane, decane, MTBE, toluene, ethylbenzene, and
o-xylene. Therefore, factor 3 was identified as multiple sources. Factor 4 was represented by a
high concentration of isopentane, n-pentane, and MTBE. Therefore, factor 4 was identified as
gasoline evaporation. Factor 5 was represented by high concentrations of benzene, therefore,
1025 identified as gasoline vehicle exhaust. Factor 6 was assigned to LPG/NG usage due to the high
contribution of propane, n-butane, and isobutane (Shao et al., 2016). Factor 7 was identified as
diesel vehicle exhaust due to the high contribution of acetylene, n-heptane, and decane.



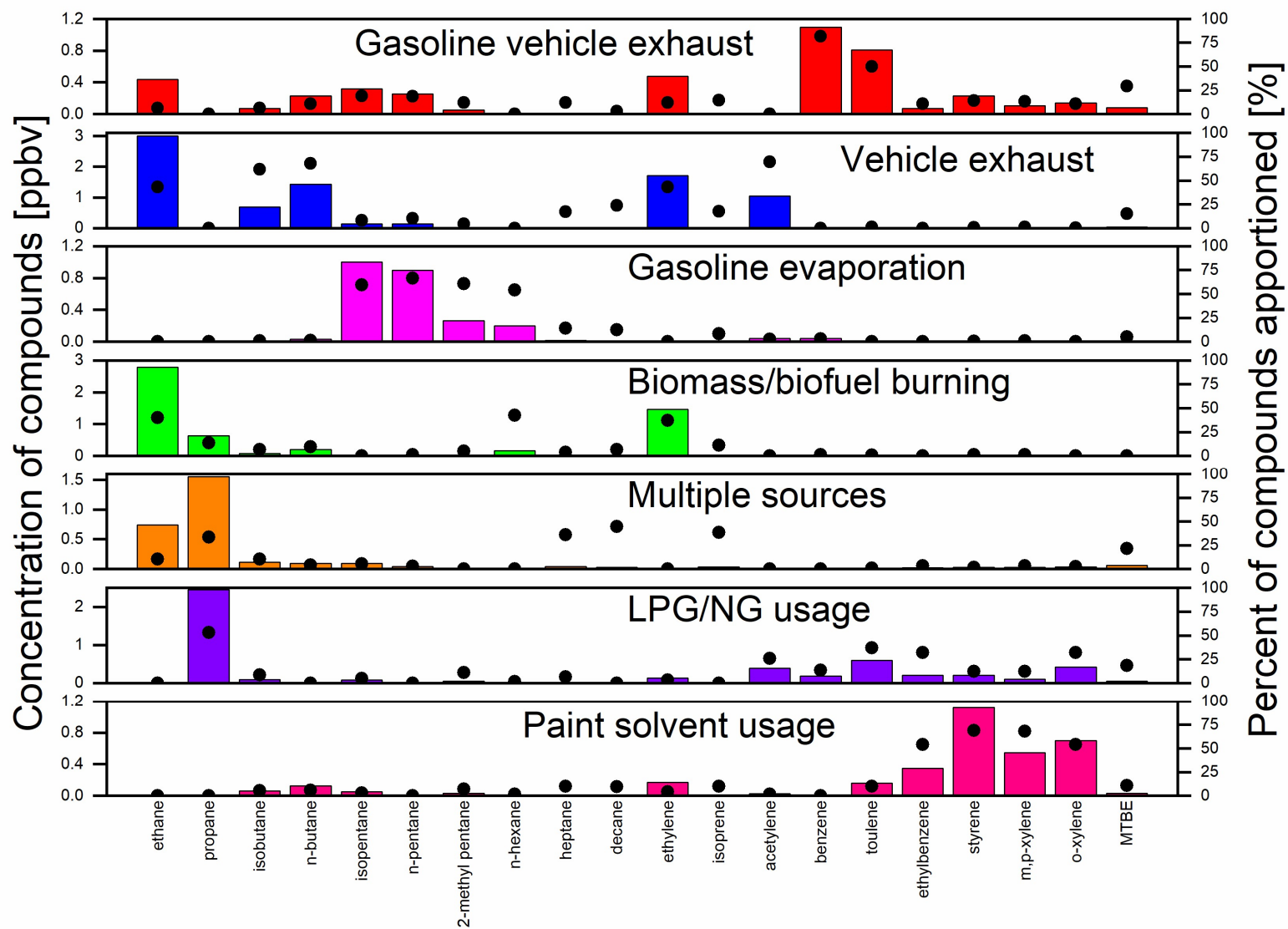
1028

1029 **Figure S1: Source profile of VOCs during summer in Nanjing industrial area**



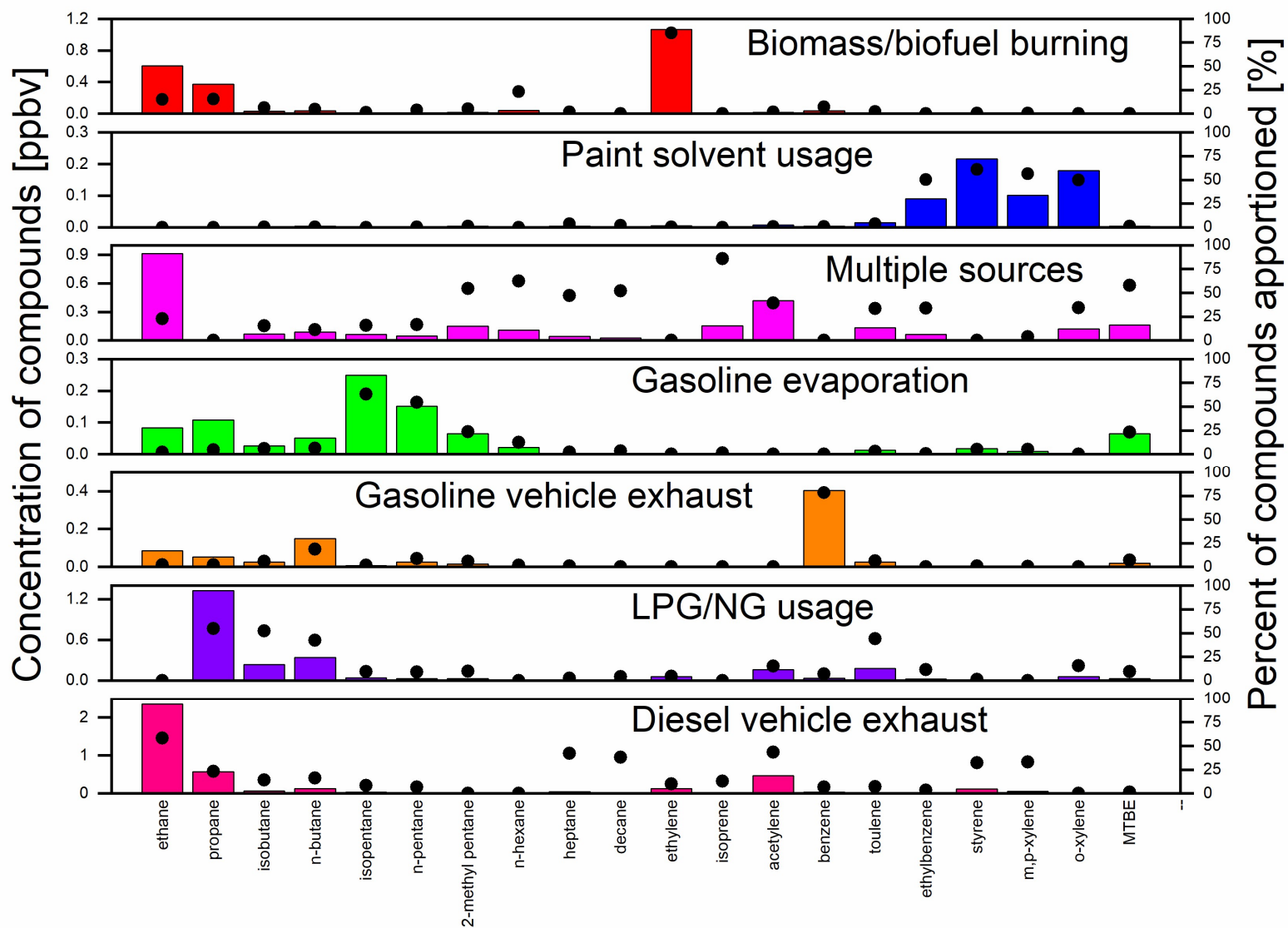
1030

1031 **Figure S2: Source profile of VOCs during autumn in Nanjing industrial area**



1032

1033 **Figure S3: Source profile of VOCs during winter in Nanjing industrial area**



1034

1035 **Figure S4: Source profile of VOCs during spring in Nanjing industrial area**

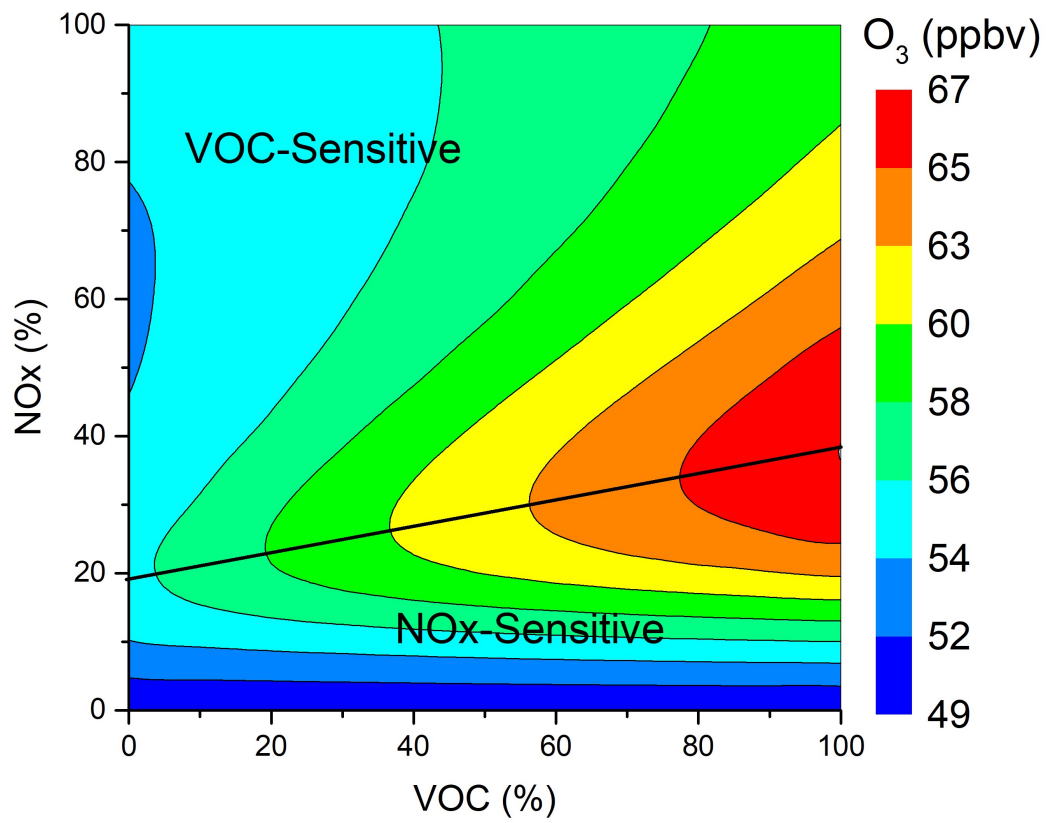


Figure S5: O₃ isopleth diagram on a high O₃ episode day (July 29 2018) in Nanjing industrial area.

1040

1045

References

- 1050 An, J., Wang, J., Zhang, Y., & Zhu, B. (2017). Source Apportionment of Volatile Organic Compounds in an Urban Environment at the Yangtze River Delta, China. *Archives of Environmental Contamination and Toxicology*, 72(3), 335–348. <https://doi.org/10.1007/s00244-017-0371-3>
- An, J., Zhu, B., Wang, H., Li, Y., Lin, X., & Yang, H. (2014). Characteristics and source apportionment of VOCs measured in an industrial area of Nanjing, Yangtze River Delta, China. *Atmospheric Environment*, 97, 206–214. <https://doi.org/https://doi.org/10.1016/j.atmosenv.2014.08.021>
- 1055 Borbon, A., Locoge, N., Veillerot, M., Galloo, J. C., & Guillermo, R. (2002). Characterisation of NMHCs in a French urban atmosphere: overview of the main sources. *Science of The Total Environment*, 292(3), 177–191. [https://doi.org/https://doi.org/10.1016/S0048-9697\(01\)01106-8](https://doi.org/https://doi.org/10.1016/S0048-9697(01)01106-8)
- Carter, W. P. L. (2010). Development of the SAPRC-07 chemical mechanism. *Atmospheric Environment*, 44(40), 5324–5335. <https://doi.org/10.1016/j.atmosenv.2010.01.026>
- 1060 Derwent, R. G., Jenkin, M. E., Utembe, S. R., Shallcross, D. E., Murrells, T. P., & Passant, N. R. (2010). Secondary organic aerosol formation from a large number of reactive man-made organic compounds. *Science of the Total Environment*, 408(16), 3374–3381. <https://doi.org/10.1016/j.scitotenv.2010.04.013>
- 1065 Dörter, M., Odabasi, M., & Yenisoy-Karakaş, S. (2020). Source apportionment of biogenic and anthropogenic VOCs in Bolu plateau. *Science of the Total Environment*, 731, 1–18. <https://doi.org/10.1016/j.scitotenv.2020.139201>
- Hui, L., Liu, X., Tan, Q., Feng, M., An, J., Qu, Y., ... Cheng, N. (2019). VOC characteristics, sources and contributions to SOA formation during haze events in Wuhan, Central China. *Science of the Total Environment*, 650, 2624–2639. <https://doi.org/10.1016/j.scitotenv.2018.10.029>
- 1070 Hui, L., Liu, X., Tan, Q., Feng, M., An, J., Qu, Y., ... Jiang, M. (2018). Characteristics, source apportionment and contribution of VOCs to ozone formation in Wuhan, Central China. *Atmospheric Environment*, 192(August), 55–71. <https://doi.org/10.1016/j.atmosenv.2018.08.042>
- Li, J., Zhai, C., Yu, J., Liu, R., Li, Y., Zeng, L., & Xie, S. (2018). Spatiotemporal variations of ambient volatile organic compounds and their sources in Chongqing, a mountainous megacity in China. *Science of the Total Environment*, 627, 1442–1452. <https://doi.org/10.1016/j.scitotenv.2018.02.010>
- 1075 Liu, P. W. G., Yao, Y. C., Tsai, J. H., Hsu, Y. C., Chang, L. P., & Chang, K. H. (2008). Source impacts by volatile organic compounds in an industrial city of southern Taiwan. *Science of the Total Environment*, 398(1–3), 154–163. <https://doi.org/10.1016/j.scitotenv.2008.02.053>

- 1080 Liu, Y., Shao, M., Fu, L., Lu, S., Zeng, L., & Tang, D. (2008). Source profiles of volatile organic compounds (VOCs) measured in China: Part I. *Atmospheric Environment*, *42*(25), 6247–6260. <https://doi.org/https://doi.org/10.1016/j.atmosenv.2008.01.070>
- Lyu, X., Guo, H., Simpson, I. J., Meinardi, S., Louie, P. K. K., Ling, Z., ... Blake, D. R. (2016). Effectiveness of replacing catalytic converters in LPG-fueled vehicles in Hong Kong. *Atmospheric Chemistry and Physics*, *16*(10), 6609–6626. <https://doi.org/10.5194/acp-16-6609-2016>
- 1085 McCulloch, A., Aucott, M. L., Benkovitz, C. M., Graedel, T. E., Kleiman, G., Midgley, P. M., & Li, Y.-F. (1999). Global emissions of hydrogen chloride and chloromethane from coal combustion, incineration and industrial activities: Reactive Chlorine Emissions Inventory. *Journal of Geophysical Research: Atmospheres*, *104*(D7), 8391–8403. <https://doi.org/https://doi.org/10.1029/1999JD900025>
- 1090 Pallavi, Sinha, B., & Sinha, V. (2019). Source apportionment of volatile organic compounds in the northwest Indo-Gangetic Plain using a positive matrix factorization model. *Atmospheric Chemistry and Physics*, *19*(24), 15467–15482. <https://doi.org/10.5194/acp-19-15467-2019>
- Reimann, S., Calanca, P., & Hofer, P. (2000). The anthropogenic contribution to isoprene concentrations in a rural atmosphere. *Atmospheric Environment*, *34*(1), 109–115. [https://doi.org/https://doi.org/10.1016/S1352-2310\(99\)00285-X](https://doi.org/https://doi.org/10.1016/S1352-2310(99)00285-X)
- 1095 Saeaw, N., & Thepanondh, S. (2015). Source apportionment analysis of airborne VOCs using positive matrix factorization in industrial and urban areas in Thailand. *Atmospheric Pollution Research*, *6*(4), 644–650. <https://doi.org/https://doi.org/10.5094/APR.2015.073>
- Shao, P., An, J., Xin, J., Wu, F., Wang, J., Ji, D., & Wang, Y. (2016). Source apportionment of VOCs and the contribution to photochemical ozone formation during summer in the typical industrial area in the Yangtze River Delta, China. *Atmospheric Research*, *176–177*, 64–74. <https://doi.org/10.1016/j.atmosres.2016.02.015>
- 1100 Song, M., Li, X., Yang, S., Yu, X., Zhou, S., Yang, Y., ... Zhang, Y. (2020). Spatiotemporal Variation, Sources, and Secondary Transformation Potential of VOCs in Xi'an, China, *30*(August). Retrieved from <https://doi.org/10.5194/acp-2020-704>
- 1105 Song, M., Tan, Q., Feng, M., Qu, Y., Liu, X., An, J., & Zhang, Y. (2018). Source Apportionment and Secondary Transformation of Atmospheric Nonmethane Hydrocarbons in Chengdu, Southwest China. *Journal of Geophysical Research: Atmospheres*, *123*(17), 9741–9763. <https://doi.org/10.1029/2018JD028479>
- 1110 Wang, G., Cheng, S., Wei, W., Zhou, Y., Yao, S., & Zhang, H. (2016). Characteristics and source apportionment of VOCs in the suburban area of Beijing, China. *Atmospheric Pollution Research*, *7*(4), 711–724. <https://doi.org/10.1016/j.apr.2016.03.006>
- Wu, F., Yu, Y., Sun, J., Zhang, J., Wang, J., Tang, G., & Wang, Y. (2016). Characteristics, source

1115 apportionment and reactivity of ambient volatile organic compounds at Dinghu Mountain in Guangdong Province, China. *Science of the Total Environment*, 548–549, 347–359. <https://doi.org/10.1016/j.scitotenv.2015.11.069>

Wu, R., Zhao, Y., Zhang, J., & Zhang, L. (2020). Variability and sources of ambient volatile organic compounds based on online measurements in a suburban region of nanjing, eastern China. *Aerosol and Air Quality Research*, 20(3), 606–619. <https://doi.org/10.4209/aaqr.2019.10.0517>

1120 Yu, C. H., Zhu, X., & Fan, Z. (2014). Spatial/temporal variations and source apportionment of VOCs monitored at community scale in an urban area. *PloS One*, 9(4), e95734–e95734. <https://doi.org/10.1371/journal.pone.0095734>

1125 Zhang, H., Li, H., Zhang, Q., Zhang, Y., Zhang, W., Wang, X., ... Xia, F. (2017). Atmospheric volatile organic compounds in a typical urban area of beijing: Pollution characterization, health risk assessment and source apportionment. *Atmosphere*, 8(3). <https://doi.org/10.3390/atmos8030061>

Zhang, Y., Li, R., Fu, H., Zhou, D., & Chen, J. (2018). Observation and analysis of atmospheric volatile organic compounds in a typical petrochemical area in Yangtze River Delta, China. *Journal of Environmental Sciences (China)*, 71, 233–248. <https://doi.org/10.1016/j.jes.2018.05.027>

1130